Publication No. 04-076-252

INDUSTRIALIZED REMOTE REAL-TIME ANALYSES OF PHOSPHATE

FINAL REPORT

Prepared by

LASER DISTANCE SPECTROMETRY
Petach Tikva, Israel

and

R SQUARED S, INC.
Lakeland, FL

under a grant sponsored by

April 2015

The Florida Industrial and Phosphate Research Institute (FIPR Institute) was created in 2010 by the Florida Legislature (Chapter 1004.346, Florida Statutes) as part of the University of South Florida Polytechnic. The FIPR Institute superseded the Florida Institute of Phosphate Research established in 1978 but retained and expanded its mission. In April 2012 the statute was amended by the Florida Legislature, transferring the Institute to the Florida Polytechnic University as of July 1, 2012. The FIPR Institute is empowered to expend funds appropriated to the University from the Phosphate Research Trust Fund. It is also empowered to seek outside funding in order to perform research and develop methods for better and more efficient processes and practices for commercial and industrial activities, including, but not limited to, mitigating the health and environmental effects of such activities as well as developing and evaluating alternatives and technologies. Within its phosphate research program, the Institute has targeted areas of research responsibility. These are: establish methods for better and more efficient practices for phosphate mining and processing; conduct or contract for studies on the environmental and health effects of phosphate mining and reclamation; conduct or contract for studies of reclamation alternatives and wetlands reclamation; conduct or contract for studies of phosphatic clay and phosphogypsum disposal and utilization as a part of phosphate mining and processing; and provide the public with access to the results of its activities and maintain a public library related to the institute's activities.

The FIPR Institute is located in Polk County, in the heart of the Central Florida phosphate district. The Institute seeks to serve as an information center on phosphate-related topics and welcomes information requests made in person, or by mail, email, fax, or telephone.

Florida Industrial and Phosphate Research Institute
1855 West Main Street
Bartow, Florida 33830
(863) 534-7160
Fax: (863) 534-7165
http://www.fipr.state.fl.us

INDUSTRIALIZED REMOTE REAL-TIME ANALYSES OF PHOSPHATE

FINAL REPORT

Michael Gaft
Principal Investigator

LASER DISTANCE SPECTROMETRY
11 Granit St., Petach Tikva 49514, Israel

with

Regis Stana

R SQUARED S, INC.
2214 Deerbrook Dr., Lakeland, FL 33811

Prepared for

FLORIDA INDUSTRIAL AND PHOSPHATE RESEARCH INSTITUTE
1855 West Main Street
Bartow, Florida 33830 USA

Project Manager: Dr. Patrick Zhang
FIPR Project Number: 12-04-076

April 2015

DISCLAIMER

The contents of this report are reproduced herein as received from the contractor. The report may have been edited as to format in conformance with the FIPR Institute *Style Manual*.

The opinions, findings and conclusions expressed herein are not necessarily those of the Florida Industrial and Phosphate Research Institute or its predecessor, the Florida Institute of Phosphate Research, nor does mention of company names or products constitute endorsement by the Florida Industrial and Phosphate Research Institute.

PERSPECTIVE

Patrick Zhang, Research Director - Beneficiation & Mining

A decade-long research collaboration between Dr. Gaft of Laser Distance Spectrometry (LDS) of Israel and the FIPR Institute has resulted in the development and commercialization of the world's first on-line analyzer (Maya) for wet minerals using the laser-induced breakdown spectroscopy (LIBS) technology. Although the original objective of the on-line LIBS analyzer was to determine dolomite content, much more has been accomplished. The commercialized analyzer not only gives dolomite readings with acceptable accuracy, but also analyzes or calculates contents of other important components such as BPL, CaO, minor element ratio (MER), Fe_2O_3, Al_2O_3 and Insol. Another nice feature of the analyzer is remote, wireless operation. The Florida phosphate industry has installed two Maya analyzers. According to an industry estimate, one installation of Maya at a phosphate beneficiation plant could bring an annual economic benefit of about $3 million.

Ore evaluation in the exposed mine face and in the dragline bucket can increase reserves by including phosphate deposits with high Mg content from southern Florida in economically viable production. Because of selective excavation and dumping, most of the dolomite will be separated near the open pit, thus reducing ore transportation costs significantly. An additional advantage may be the lowering of energy use and flotation chemical consumption, because ore with excessive contaminants will be removed before expensive grinding and flotation processes.

The FIPR Institute and the Israeli research team have long set the goal of developing a LIBS-based analyzer for remote analysis of ores and overburden before these materials are dug out or have begun transit to the beneficiation plant. The many years of research and successful deployment of the on-line analyzer have laid a sound foundation for developing a remote LIBS, which can provide analogous information at a much greater distance from the target rock.

Under phase one of the remote LIBS program, distant evaluation in the lab and field testing of a remote LIBS prototype demonstrated its feasibility for distant (from 5-25 m), real-time chemical analysis of phosphate minerals excavated by the dragline. Analytical data from the remote LIBS correlated well with laboratory analyses, giving a correlation coefficient of $R^2 = 0.915$ for P_2O_5 and 0.75 for MgO. In the current project, an industrialized unit was constructed and tested, capable for constant functioning in real-life conditions of the open phosphate mine. The unit proved to be robust, and gave reliable and useful information on phosphate matrix during the course of its discharge from dragline bucket to the slurry pit. However, it was determined that in order to take full advantages of remote analysis, the analyzer would have to be mounted on the dragline, which is a big engineering challenge requiring further funding beyond the means of this Institute.

ABSTRACT

LDS (formerly Laser Detect Systems, now Laser Distance Spectrometry) earlier constructed and produced an industrial LIBS machine, which enables online measurement of the Mg, Fe, Al, Si, Ca and P_2O_5 content of phosphate rock on a moving conveyer belt. It allows real time shipping and discarding decisions based on sound analytical data. Two LIBS machines are working in the Florida phosphate industry (Mosaic). While this allows for sorting of phosphate rock after mining pumping and separation, there is an advantage to doing the rock characterization much sooner in the process, not only to eliminate the cost of mining, pumping and separation, but also to reduce the possibility of discarding good rock rather than mining it. This required the construction of a remote LIBS unit capable of identifying rock quality from a distance of up to 25 meters. To prove the feasibility of a remote real-time LIBS analyzer of phosphate rocks that could be used for rock analysis at the mine face, rock in the dragline bucket or rock prior to sluicing it into the pumping pit, LDS constructed and successfully tested in real field conditions a remote LIBS (ReLIBS) unit capable of performing phosphate rock analysis at 5-25 m distances. As a next step, an industrialized unit was constructed and tested, capable of constant functioning in the real-life conditions of an open phosphate mine. This remote LIBS device proved the feasibility of distant real-time chemical analysis of phosphate rocks excavated by dragline machine in that it:

1. Differentiated between overburden, matrix and bottom materials
2. Determined the P_2O_5 content
3. Determined the MgO and iron content in the matrix samples
4. Initially, the optimum position (considering safety and mechanical feasibility) of the ReLIBS was determined to be at the washing pit before the matrix is slurried with water to pump to the beneficiation plant

After successful field testing of the machine, it was determined that a more optimum location would be on the dragline boom, looking down at the contents of the dragline bucket prior to dumping of its contents.

ACKNOWLEDGEMENT

We express our gratitude to Dr. Chaucer Hwang for his great contribution to this project.

TABLE OF CONTENTS

TABLE OF CONTENTS (CONT.)

LIST OF FIGURES

Figure **Page**

LIST OF FIGURES (CONT.)

Figure **Page**

LIST OF FIGURES (CONT.)

Figure **Page**

EXECUTIVE SUMMARY

Variability in the phosphate rock significantly affects the ability to efficiently digest the rock in the phosphoric acid production plant and produce a saleable phosphate fertilizer product. The most significant variables are the CaO, MgO, Fe_2O_3 and Al_2O_3 as well as the P_2O_5 content. Current practices require either holding the rock products in bins until the quality control data from sampling become available, or making the shipping or discarding decision based on visual observations of rock. This practice can result in the shipping of undesirable products to the chemical plant or the discarding of acceptable pebbles.The method of improving variability would be to continuously analyze the rock received by the production plant and then stack it in places on the pile with similar compositions. Then rock could be retrieved from the pile by pulling from various places on the pile to hold the overall composition relatively constant. While this would significantly improve the variability, it will only become practical when a continuous analyzer becomes available that can accurately and quickly provide the several analyses required on the rock as received without sample preparation. Online and automatic analysis allows phosphate producers to promptly detect changes in incoming materials, enabling them to take appropriate actions in the process streams.

Together with FIPR, LDS has already developed an online LIBS analyzer for phosphate rock on a moving belt conveyer. Two such machines are working in the Florida phosphate industry (Mosaic). However, it will be even more effective to put the online analytical system in the actual mine. The main opportunity would be to use it for horizon control in open mining. Presently areas to be mined are identified by geologists based on analysis of drill cores typically collected at 100 meter intervals. If field samples are collected, they must be transported to the laboratory, analyzed, and the data transmitted back to the mine. This latter process is slow, error prone, and does not allow real-time management of mining. Costs can be significantly reduced by in-situ element analysis, enabling real-time selection of the highest-grade ore. The best way to solve this problem may be to find the indistinct top and bottom contacts between barren, apatite and dolomite layers and thereby accomplish crude separation by means of selective excavation. It may be accomplished by horizon surface scanning using LIDAR (Light Detection and Ranging) system for in-situ real time phosphate-dolomite identification.

As a next stage**,** the feasibility of using a remote real-time analyzer of phosphate rocks, which could be used to analyze rock at the open mine was proven. LDS constructed and successfully tested in real field conditions a remote LIBS (ReLIBS) unit capable of analyzing phosphate rock from distances of 5-25 m. The ReLIBS device proved the feasibility of distant real-time chemical analysis of phosphate minerals excavated by the dragline machine and provided differentiation between overburden, matrix and bottom materials; measurement of P_2O_5 content; and measurement of MgO content in the matrix samples. The optimal position for the devise at that time was determined to be the washing pit where the matrix is piled prior to slurrying for transportation to the beneficiation plant.

The aim of the new project was to produce an industrialized ReLIBS unit which would be capable of working continuously in the real-life conditions of an open phosphate mine, which include a dusty/dirty atmosphere, varying temperatures, scanning in the presence of strong sunlight, and improved analytical performance, including direct detection of P in the mineral apatite using plasma emissions from the CaF molecules.

The basic stages of the present project were:

- Laboratory-scale remote experiments and optical design;
- Construction and testing of a product prototype at laboratory scale;
- Optimization and correction of parameters using laboratory tests;
- Feasibility proving of the product prototype in Florida for remote detection under field conditions.

As a result, LDS constructed and successfully tested under real field conditions a remote LIBS (ReLIBS) prototype unit capable of phosphate rock analysis from distances of 5-25 m. The ReLIBS device proved the feasibility of distant real-time chemical analysis of phosphate minerals excavated by the dragline machine and provided differentiation between overburden, matrix and bottom; measurement of the P_2O_5 contents; and measurement of MgO content in matrix samples. The preferred location for the device was found to be the washing pit where the matrix is piled prior to slurrying with water for transportation to the beneficiation plant. All testing for the project was carried out at this location. After successful field testing of the machine, it was determined that a more optimum location would be on the dragline boom, looking down at the contents of the dragline bucket prior to dumping of its contents.

INTRODUCTION

BACKGROUND

Optical sensing techniques provide the capability to remotely monitor and measure different natural objects, specifically minerals, by directing a laser beam across a long atmospheric path length to the target. The wide applicability is feasible due to the fact that the information is gained from the light received by a receptor which commonly measures absorption or scattering of the probe beam, or fluorescence or Raman radiation emitted by the corresponding minerals and rocks (Gaft and others 2005). LDS research demonstrated that laser-induced time-resolved luminescence is not efficient for effective separation between different minerals typically in the Florida phosphate rocks. We also studied Raman spectra of those minerals and arrived at the conclusion that Raman spectra are not suitable for the task. Laser-induced breakdown spectroscopy (LIBS) was found to be the best technique to differentiate remotely between the relevant minerals. This was commercialized in a LIBS industrial machine, which is now being effectively used for online control of phosphate rock on a moving conveyer belt. In this application, the phosphate rock is analyzed and all low quality rock is discarded effectively improving the quality of the rock used for the production of phosphoric acid. However, at this point in the mining process, a significant cost has been incurred for the production of the discarded rock. It would be more effective to put the online analytical system closer to the initial mining rather than on the conveyer. The first opportunity would be to use the analyzer to look at the mine face or as it is removed from the mine face. Presently areas to be mined are identified by geologists based on analysis of drill cores typically collected at 100 meter intervals. If field samples are collected, they must be transported to the laboratory, analyzed, and the data transmitted back to the mine. This latter process is slow, error prone, and does not allow real-time management of mining. Mining costs can be significantly reduced by in-situ element analysis enabling real-time selection of the highest-grade ore. The best way to solve this problem may be to find indistinct top and bottom contacts between overburden, apatite and dolomite layers and thereby accomplish at least preliminary crude dolomite separation by means of selective excavation.

Some potential hazards associated with standoff LIBS are the following. Laser light poses an ocular and skin hazard and special care must be taken. Common sense and safety regulations, such as ANSI Z136.1 (ANSI 2000), provide accepted rules. The Laser Institute of America in Orlando, Florida, has information regarding laser safety, safety training to minimize exposure to laser radiation. High voltages (e.g., laser power supplies) are potentially hazardous. Personnel are protected from high voltages and electric shock by interlocks and grounded metal shielding. These hazards are similar to those for LIBS conveyer analyzer. In the case of the ocular laser hazard, special safety goggles provide 100% protection from the laser beam.

LITERATURE REVIEW

LIBS standoff mineralogical applications have been considered mostly for space tasks. The main reason is that elements' LIBS signals depend on atmospheric pressure and are approximately 2-4 times stronger in airless locations, such as Mars and the moon, as compared to in the earth's atmosphere. Nevertheless, even for atmospheric pressures remote distances of 10-25 m have been achieved. Excellent LIBS ability for remote sensing was demonstrated in homeland security applications, where the detection and identification of trace amounts of explosives at distances up to 45 m using remote LIBS have been demonstrated (Cremers and Radziemski 2006; Gaft and Nagli 2008; Noll 2012; Palanco and Laserna 2004; Sallé and others 2007). This development clearly indicates that LIBS sensors can be made rugged, compact, and can be excellent candidates for mining robotics applications.

Laser Distance Spectrometry (LDS) is involved in developing industrial LIBS units, specifically for mining applications. LDS has vast experience with LIBS on minerals, specifically with Florida phosphate rocks, coal, and potassium fertilizers (Gaft and others 2002; Gaft and Nagli 2004; Gaft and others 2007; Gaft and others 2008; Gaft and others 2009; Groisman and Gaft 2010, Gaft and others 2014a). Our accumulated experience gives means to evaluate the feasibility of remote LIBS analysis of phosphate rocks in the exposed mining conditions.

To our knowledge, no one else presently uses LIBS as a method for mineral remote sensing, neither generally, nor specifically for real-time analysis of phosphate ore with high dolomite content.

PURPOSE OF THE PROJECT

According to previous field experiments, it was concluded that the following changes had to be made in order to improve the device's abilities.

The spectrometer used was not optimal. The gating time of 1 ms is not enough in order to eliminate totally the strong sunlight emissions and when it strikes directly on the target the broad spectral band is detected, interfering with the plasma emissions. In order to remove this interference, the gating time has to be narrower, down to 10-100 μs. In such a case, the signal from a constant source, such as the sun, will be substantially lower, while the LIBS signal with its lifetime of 5-50 μs remains nearly the same.

The main elements taking part in the analytical algorithm are Ca, Mg, Fe, Si and Al. All those elements are much easier to detect in the UV and not in the visible spectrum. According to our accumulated experience, a range of 240-320 nm is optimal for this specific task. The spectral resolution has to be twice as good compared to present spectrometers. All these requirements had to be fulfilled by the new device.

The previous MAYA operating units use a single pulsed LIBS laser, which has 100 mJ/pulse energy. In order to make the plasma stronger and the sensitivity correspondingly higher, a double pulsed LIBS technique was applied (Cremers and Radziemski 2006; Miziolek and others 2006) with two lasers with 100 mJ/pulse energy.

The profile change is relatively large, thus the device has to be equipped with a distance measuring device and the ability to autofocus the optical system in accordance with changing distance between the device and target.

METHODOLOGY

LASER INDUCED BREAKDOWN SPECTROSCOPY

LIBS is a well-known laboratory technique commonly used for fast elemental analysis of materials. Its methodology relies on the capability of high-power lasers to ablate a certain amount of material from a sample surface and the simplicity of the setup required to perform atomic emission spectrometry on the emitting plasma. Threshold irradiance to induce plasma formation is on the order of 10^9 W/cm^2 for most solids. This level is several orders of magnitude higher than those commonly employed by regular remote sensing techniques where the laser beam is directed unfocused towards the target [Laser Induced Luminescence (LIL), Raman]. Consequently, special care must be paid to tightly focus the beam in order not only to reach the plasma formation threshold, but to produce sufficiently bright plasma of analytical quality. This has only been attainable with the development of pulsed lasers capable of producing short pulses of high energy with high stability and low divergence. Additionally, in contrast with LIL and Raman spectroscopies where the analyzed spot may be relatively large, laser-produced plasma is a light source of a few millimeters. In addition, laser-induced plasmas are high-intensity radiating sources, usually an order of magnitude stronger that luminescence and especially Raman signals. The human eye can detect the emission from laser induced plasma from a distance of several tens of meters in the daylight. As was already mentioned, the 10^8-10^9 W/cm^2 regime light interaction with matter is characterized by the formation of a high temperature and electron dense plasma, useful for determining the chemical species which constitute the original sample. Since laser-induced plasmas are pulsed sources, their excitation features are a function of time. During the first stages after plasma formation, the emission spectrum is dominated by an intense continuous emission background due to recombination and bremmstrahlung. As plasma decays, the intensity of background and doubly ionized ions significantly decrease due to a decrease in temperature and electron density, and line emission due to single ionized and neutral species becoming detectable. Owing to the strict energy requirements of the plasma formation process, and occasionally to shielding of the laser radiation by the plasma, the amount of the ablated sample can be in the range of 10^{-9}–10^{-6} g per pulse depending on the characteristics of the laser source, the physical properties of the sample, and its surface state. In general, the ablated mass increases with pulse irradiance and sample temperature and decreases with surface reflectivity and the sample thermal conductivity and latent heat of fusion and vaporization. Detection limits achieved by the technique are commonly in the parts per million levels. The analysis principle for laser-induced plasmas is similar to those of other techniques based on atomic emission spectrometry. The plasma light is spectrally and time resolved to identify the light-emitting species. The execution of a measurement implies the integration of the signal corresponding to a line or group of lines of the elements of interest over a certain period of time. The quantity of the element is determined by building a calibration curve of the signal versus the concentration in samples of known composition.

Unit Development and Production

UV Spectrometer

Figure 1 presents plasma emission spectra of apatite and dolomite from the Mosaic South Pasture mine in UV range measured in remote mode. All relevant elements, such as P, Mg, Si, Al, Fe and Ca are clearly seen with very high Signal/Noise (S/N) ratio. In real field experiments, the measuring distance of 30 m will be 4 times greater. In order to compensate for the corresponding decreasing signal, the collecting mirror diameter had to be 4 times larger, namely approximately 30 cm.

Double Pulsed (DP) LIBS

The way to improve LIBS analytical abilities is to use a double pulsed (DP) LIBS. It is conducted by using two pulses from two laser sources operated at either a single or at different wavelengths. By utilizing a commercial DP laser system, a proper external trigger circuit can extract two laser pulses with an adjustable delay between the pulses, variable from 10 nanoseconds to several tenths of microseconds. The experimental results show that such technique increases significantly the intensity of spectral lines in the emission spectrum from the near-surface plasma. This enables a significant increase in the sensitivity of this technique when applied to remote analysis. Another possible advantage of the double pulse technique is also related to the cleaning action produced by the first laser pulse, which can have positive effects in applications where samples with dust and coatings are not cleaned. LDS has already successfully used DP LIBS in several online LIBS analyzers where the analytical signals with single pulsed (SP) LIBS were relatively weak.

Figure 2 presents a comparison between SP and DP signals from Mosaic South Pasture apatite rock. It may be seen that the intensity of all lines are 5-10 times larger, depending on the corresponding element and its ionization. For example, P I emission lines become 6 times stronger. It corresponds to our experience with phosphate rocks from the Kovdor phosphor-iron deposit, Russia, where P has to be analyzed while its concentration is relatively low (P_2O_5 from 5-10%) and SP LIBS does not give good results.

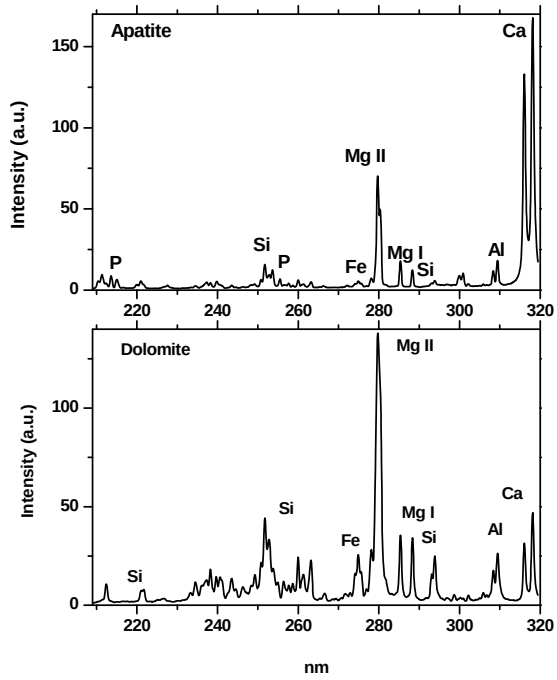

Figure 1. Breakdown Spectra of Mosaic South Pasture Apatite and Dolomite in UV Range Measured from 10 m Distance.

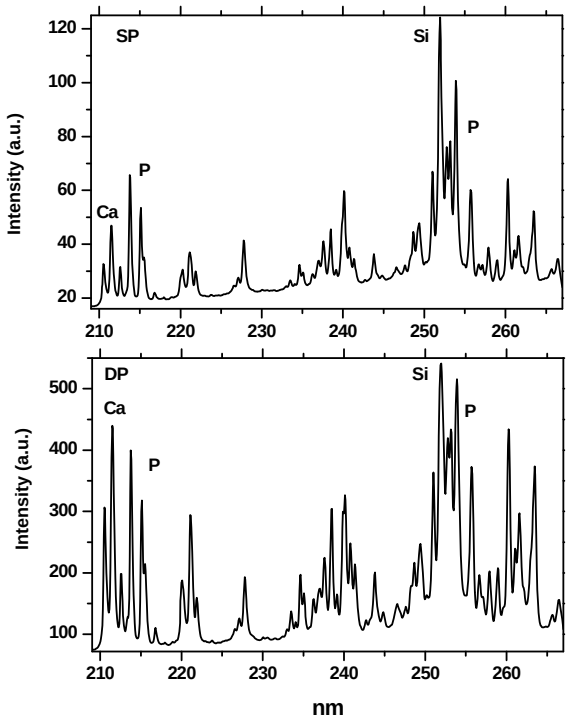

Figure 2. Comparison of Single Pulse and Double Pulse LIBS Signals for Mosaic South Pasture Phosphate Rock.

Spectrometer with Narrow Gate

All spectrometers used in LDS industrial LIBS units are of the CCD gated type, with regulated delay time and constant gate width of 1 ms. This type of online conveyer analyzer is acceptable where the working area is shielded from direct sunlight, but not for remote applications in ambient daylight conditions. As it was demonstrated during the previous project stage, the sun background interferes with the plasma emission, making analysis more difficult. The energy received in the visible spectral range from the sun at the earth's orbit by 1 m^2 in 1 s is equal to 1360 J. The spectrometer slit area is 0.1 mm^2, which corresponds to approximately 136 µJ. During a period of 1 ms, our spectrometer receives 136 nJ, which is comparable to the visible LIBS intensity. It was concluded that such background interference has to be reduced by at least one order of magnitude, namely to use a gate width of 100 µs. The task is easier in the UV spectral range where the sun background is lower than in the visible part of the spectrum. CCD gated spectrometers with a gate width of less than 1 ms are relatively new on the market. Figure 3 presents the test results of such a spectrometer, where SP plasma of the Mosaic South Pasture phosphate rock was measured using a background of a strong Hg lamp with a quartz bulb, which imitated the sunlight. With a gate width of 1 ms, two strong Hg lines were detected, peaking at 253.7 and 312.5 nm. The line at 253.7 was strongly saturated. With a gate width of 10 µs, the plasma remained strong, while the Hg lines were substantially weaker. Nevertheless, the strongest line interfered with the P lines in 253-255 nm range. It was concluded that a narrow gating ability will work and the sun background can be removed in real field applications.

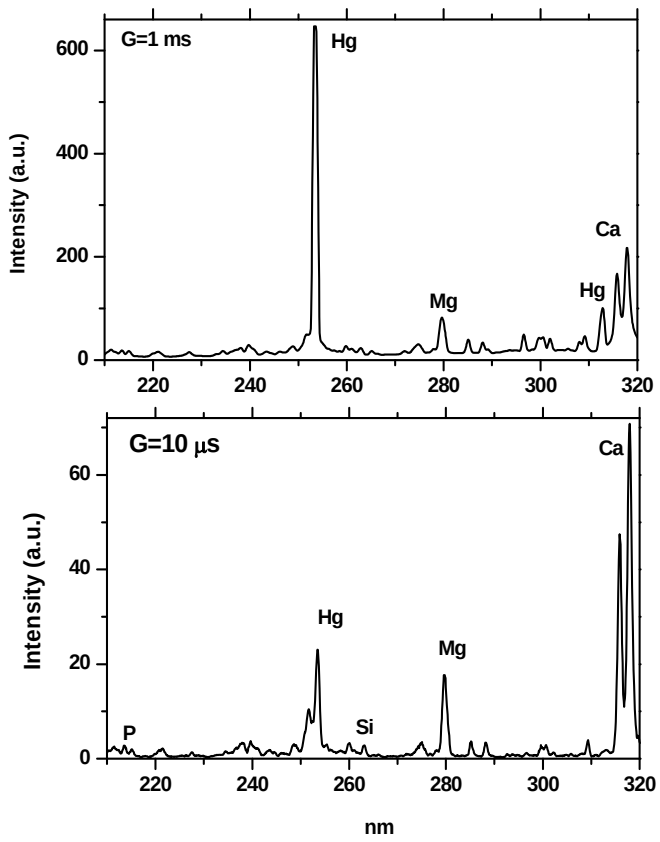

Figure 3. Comparison of Pulsed Plasma and Constant UV Source (Hg Lamp) with Different Gate Widths of 1 ms and 10 µs.

Optical Design

The following main specifications were determined for the UV ReLIBS unit design (Table 1). One of the main questions was to calculate the effective focal length to achieve the desired power density at the target. The obscuration accounts for 6% of the beam, so due to this alone the power transfer is 94%. The laser optical path was the following:

1. Transmission through two lenses of a beam expander – assume a power transfer through each lens of 99%.
2. Transmission through a dichroic beam combiner – assume a transmission coefficient of 96%.
3. Reflection off a protected aluminum scraper mirror – assume a reflectivity of 92.5%.
4. Reflection off a large concave protected aluminum mirror – assume 92.5%.
5. Reflection off a large scan protected aluminum mirror – assume 92.5%.
6. Transmission through the front window – assume 98%.

Therefore the overall power transfer is 68.6%.

If the full angle beam divergence is θ containing 86.5% of the power, then the spot diameter containing 98.5% of the power will be given by 1.5θf, where f is the effective focal length of the optical system. The power density is calculated by dividing the power by the area of the spot. For these calculations it was assumed that all the power is uniformly distributed over the full spot diameter (3ω). Two alternatives to this calculation are either the full power within the spot diameter of 2ω, or 86.5% of the power within the spot diameter of 2ω. This case with the full power contained within the 3ω spot is the worst-case scenario. The radius of the spot *r* to achieve the required power density of 3×10^9 W/cm^2 is given by:

$$r = \sqrt{\frac{0.686 \times 100 \times 10^{-3}}{8 \times 10^{-9} \times 3 \times 10^{9} \times \pi}}$$

where 0.686 is the 68.6% power transfer of the optics, 100×10^{-3} is the energy of the laser, 8×10^{-9} is the maximum pulse duration of the laser, and 3×10^9 is the required power density. From this, $r = 0.030$ cm or 0.30 mm.

As explained above, this radius is for the 98.5% spot and the radius of the spot containing 86.5% will be 0.20 mm. To achieve this spot radius, different system focal lengths will be required depending on the laser divergence angle. If the laser divergence angle is 1 mRad, then the effective focal length to achieve the required spot size will be *f*, where: $1 \times 10^{-3} f = 0.40$. From this, the designed focal length $f = 400$ mm.

Another issue is the scraper mirror diameter. The diameter of the beam expanded parallel beam has been chosen at 22 mm, which is the 3ω diameter. The reason for such a large diameter is that the scraper mirror coating has to reflect both the laser at 1064 nm and the collection beam in the wavelength region between 240 and 380 nm. It is evident that a dielectric coating is unsuitable and an enhanced aluminum coating is necessary. The damage threshold of enhanced aluminum is about 0.3 J/cm^2 for 20 ns pulses at 1064 nm. Assuming the 100 mJ pulse energy and a 2ω diameter of 14.7 mm, then the energy density at the scraper mirror surface will be 0.04 J/cm^2.

Looking at the above curve the peak intensity is 48.4 W/mm^2. This is for a power of 0.936 watts. This is equivalent to 5171 W/cm^2. Assuming a M^2 of 2.0, then the full diameter spot will be twice as large and the power density ¼. Therefore the actual power density for the 0.936 watts will be 1293 W/cm^2. Assuming a worst-case pulse width of 8ns, and a power transfer of 68.6% (see page 2), then the expected peak power density will be given by:

$$PowerDensity = \frac{0.686 \times 100 \times 10^{-3}}{8 \times 10^{-9} \times 0.936} \times 1293$$

The worst-case (lowest) peak power density is 1.18×10^{10} W/cm^2.

Table 1. Main Specifications.

Laser wavelength	10064 nm
Energy per pulse	200 mJ (2 × 100 mJ)
Pulse width	7 ns (from 6 to 8 ns)
Raw beam diameter	4 mm (assumed to be 3ω)
Laser M^2	1.968
Laser equivalent full field divergence	1.0 mRad (86.5% of the power)
Working range	From 15m to 24.6 m continuous
Power density at 24.6 m	$> 3 \times 10^9$ W/cm^2
Concave mirror diameter	300 mm
Concave mirror clear aperture for laser beam	292.5 mm (at 26 m working distance)
Overall height of system	Approx. 1300 mm (from mirror to mirror)
Effective focal length	400 mm (for 24.6 m working distance)
Collection optics wavelength	$240 < \lambda < 380$ nm
Collection optics object diameter	3.0 mm at 24.6 meters range
Collection fiber diameter	600 μm
Collection numerical aperture at object	0.00566
Collection numerical aperture at image	0.0569
Mirror clear aperture for collection	294 mm (at 24.6 m working distance)

Mechanical Design

The selected concept was chosen according to both the demands of the demands and field experience accumulated during development and testing of the feasibility proof system. In order to make the remote system as flexible as possible, the system has two separate major components (Figure 4): M-2021 (telescope), and M-1000 (utility box).

The M-2021 contains all the optical elements and their mechanics and mechanisms. The M-1000 contains the controls and monitors for the telescope. The mechanical design of the telescope was determined by three major criteria:

1. Safety of use.
2. Maximum flexibility possible, in terms of the ambient conditions (rain, heat, dust, etc.) and of the material's status and composition.
3. Ease of use.

The telescope's physical dimensions are: length, 2 m; width, 1.25 m; height, 1.1 m. It is equipped with motors to enable rotation and elevation for the scanning procedure (Figure 5).

1. Rotation range designed to cover 20 m (+/- 10 m) at target distance of 20 m (~ 65 feet).
2. Elevation range designed to cover 4 m (+ - 2 m) at target distance of 20 m. The telescope interior is very complicated and incorporates the following major items:

    a. Two laser heads
    b. Two spectrometers
    c. Laser distance meter
    d. Camera
    e. About twenty optical elements
    f. Focusing mechanism
    g. Motor controllers
    h. Heaters
    i. Chiller
    j. Fans
    k. Blowers

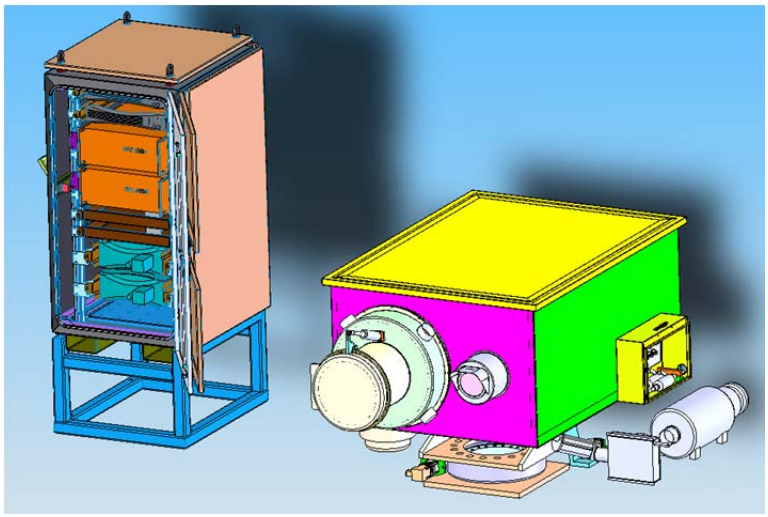

Figure 4. Full System View.

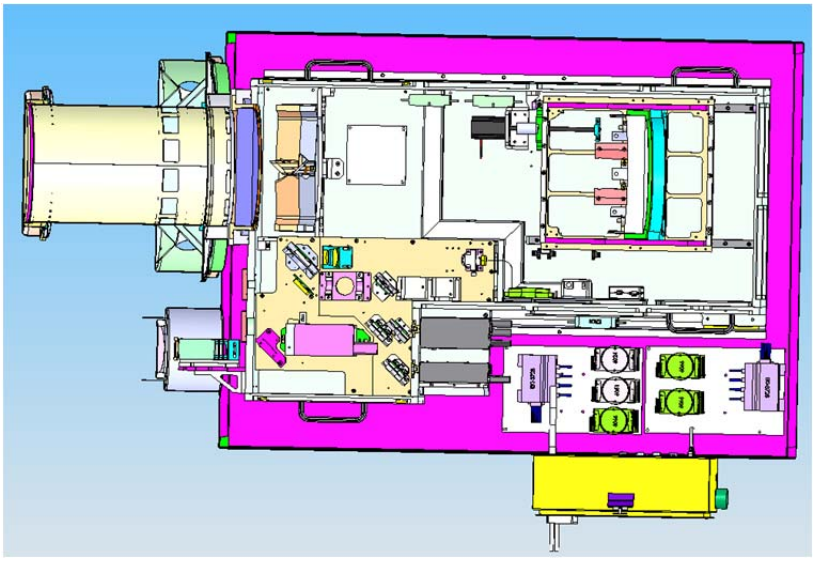

Figure 5. Telescope, Interior View.

The physical dimensions of the utility box (Figure 6) are: height with supporting frame, 1.8 m; width with connection box, 0.9 m; and depth with air conditioner, 1.4 m.

It is actually a cabinet for all the equipment needed to support the telescope's operation. It was designed with these criteria in mind:

1. Safety
2. Robustness
3. Continues work
4. Flexibility.

The utility box contains the following major systems:

1. Two laser power supplies
2. Two UPS systems
3. DC drawer
4. DC power supplies drawers
5. Industrial PC
6. Air conditioner
7. Heater
8. AC panel
9. Connection box
10. Filters.

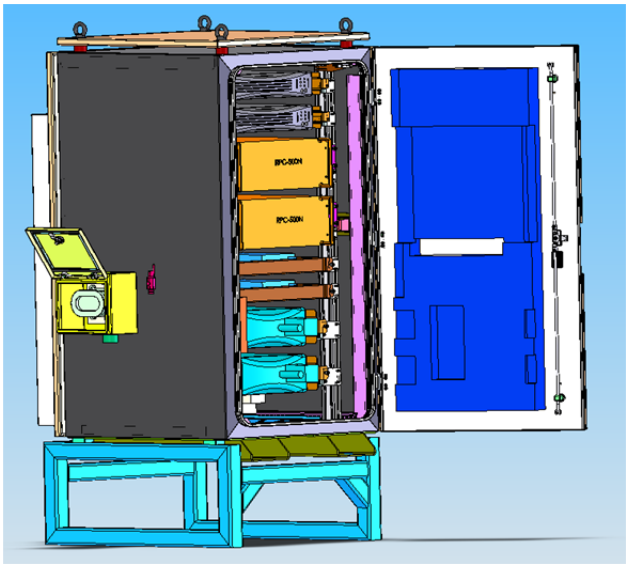

Figure 6. Utility Box, Side View.

Electrical Design

The system is divided into sub-assemblies/systems:

- The M1000 (utilities cabinet)
- The M2021 (telescope)
- Accessories

The M1000 integrates:

- AC panel.
- Controller (industrial computer)
- Laser power supply (+ liquid cooling system)
- AC-DC power supply
- Temperature stabilizing elements (heating/cooling)

The M2021 integrates:

- Lasers (Nd:YAG laser, laser pointer, laser distance meter)
- Spectrometer/s
- Lenses/mirrors
- Focusing mechanism
- Video camera
- Pan/tilt motors and controllers
- Temperature stabilizing elements (heating/cooling)

Accessories include:

- Blower (used to keep lasing window clean)
- Cyclone (used to “clean” air used by the blower)
- Heating/Cooling unit (used to stabilize M2021 internal temperature)

Interface

The interface design is as follows:

- Site:
    - Main power supply required (three phase, 400VAC, XX volt-ampere)
    - User remote control via remote control software over ethernet (TCP/IP)
    - General I/O
    - Sub assemblies:
        - Nd:YAG laser timing and coolant lines
        - LAN cable (general control and data transfer)
        - I/O cable (critical control/feedback lines)
        - AC/DC cables (mains and DC power supply)

Operating Software

Background:

- System utilizes an industrial computer
- Operating system – Windows7
- Control and analysis software – produced by LDS
- Control and analysis software automatic start-up upon computer startup
- Control and analysis software remote control/monitor – via remote control software over standard ethernet LAN (TCP/IP)
- A remote user can monitor target zone by the integrated video camera setup. During setup, remote user defines:
    - Scan pattern and resolution
    - Scan zone limits (up/down/left/right) – which are obviously within the mechanical safety limits that are set during system installation)

- A remote user aims the telescope at the starting point and initiates the sampling/lasing process
- During the sampling process
    - The telescope automatically scans the defined area. (pan/tilt)
    - At each sampling point an auto focus process is performed according to the measured target distance
    - After focusing is accomplished, the exciting laser is activated
    - At each laser pulse the spectrometer receives spectra, which are transferred for analysis by the analysis software

- General analysis results are displayed on the screen (option: target zone mapping)
- Analysis results are automatically saved into the SQL Express DB (using the system computer).

Analytical results can be read by the user:

- By ODBC interface
- By OPC MODBUS TCP/IP (optional)

The main screen (Figure 7) includes several zones:

- Header zone

    - Information: software version, algorithm description, site description, system S/N
    - Buttons: software settings, user selection (user/tech), help

- Main zone

    - Camera view (+ zoom in/out buttons) → at sampling end, turns to a Go/No-Go indication
    - Pan/tilt control (+ limit indication)
    - Measured distance

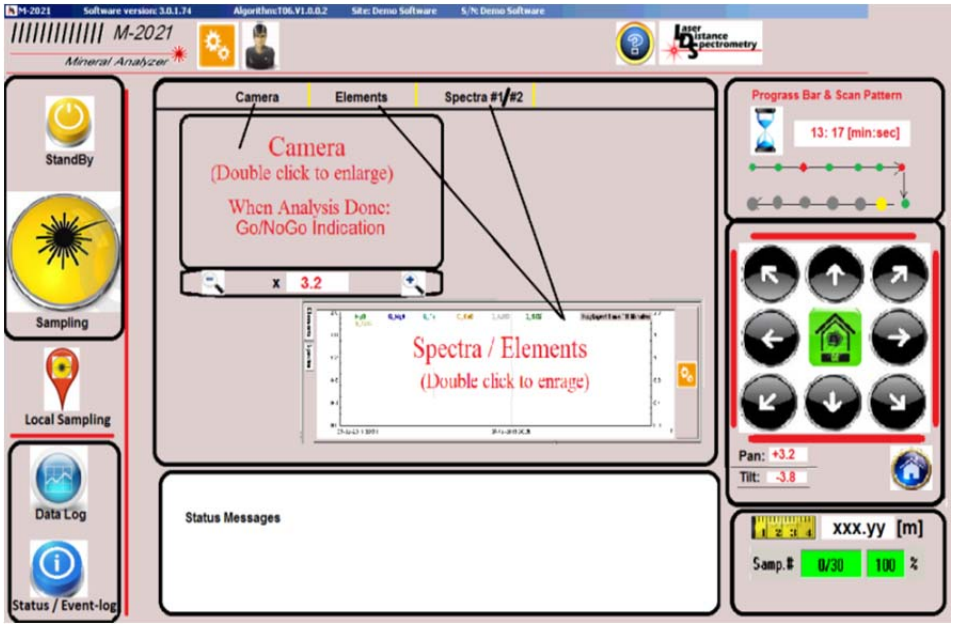

Figure 7. Main Screen.

Autofocus and Scanning

The target profile change in a real-life working scenario is always big, thus the present device was equipped with a distance measuring device and the ability to autofocus the optical system in accordance with the changing distance between the device and target. Previously, manual focusing was performed. Additionally, a scanning ability was added, enabling the measurements at a single location or by automatic scanning with selected pattern modes.

Temperature Control and Dust Protection

The ReLIBS system is equipped with air conditioning to cool the electrical part of the equipment and with a chiller and water cooling system to cool the lasers and optical module elements. Compressed air is constantly fed in order to defend the optical module window from dust and splashes from equipment working in the field. During this testing period there were not any overheating, dust or vibration-connected problems.

LABORATORY-SCALE TESTING

ReLIBS from 10 m Distance

During the initial development, the optical module of the remote system working in double pulse mode was tested in laboratory conditions using mine samples received

from Florida and other phosphate deposits all around the world. The main spectroscopic difference from the previous ReLIBS system, tested in 2011, was the combination of UV and visible spectral ranges enabling the detection of atomic P and molecular CaF emissions. This is the first ability to detect the phosphate element directly, and not indirectly, as before, and also to detect the combination of Ca and F, which is typical only for apatite in Florida phosphate mineralogy. CaF molecular emission in laser-induced plasma was recently proved by LDS and proposed for phosphate deposits analysis (Gaft and others 2014b). In both spectra ranges, the spectrometers may be changed according to the specific customer needs.

In the first stage of this test, breakdown spectra of several minerals typical for different phosphate deposits were studied. Figure 8 presents breakdown spectra of apatite with characteristic emission lines of P I peaking at 253.3 and 255.2 nm (Figures 8b, 8c) and emission band of CaF peaking at 603 nm. All other emissions are connected with Ca I and Ca II lines. Previous experience has shown that two elements, Si and Fe, may interfere with P I detection because they have strong emission lines in the same spectral range. Figure 9 presents UV breakdown spectra of Si, with the main emission lines at 251 and 288.0 spectral ranges. It may be seen that at the spectral resolution of our optical detection system emission lines of Si I and P I may be definitely separated and identified.

Figure 10 demonstrates breakdown spectra of the iron bearing mineral hematite. It is seen that Fe emission lines actually prevent P I detection in the 253-255 nm range if the iron concentration is high and phosphorus concentration is low. Fortunately, this situation is not typical for Florida phosphate deposits and Fe lines are weak relative to strong P I emission lines and do not prevent its detection. The iron-phosphorus Kovdor deposit in Russia is known for high hematite and low apatite concentrations and in that case P I emission line detection has to be done at the 215-220 nm spectral range, where Fe emission is relatively weak and spectrally separated from P I lines. The main potential obstacle for CaF molecular band emission is CaO bands typical for apatite and calcite (Figure 11). Nevertheless, they are spectrally separated in our optical detection system. Optimally they may be seen in the breakdown spectra with a long delay time of 15 μs (Figure 12) because molecular emissions have very long plasma lifetimes, much longer than Ca I and Ca II atom and ion emissions. Thus after such a delay they dominate the breakdown spectra. Another very important element for phosphate rock online analysis is Mg, the main form of which is dolomite. Double pulse breakdown spectra of dolomite demonstrate the well-known emission lines of Mg in the visible 517.8 nm and ultraviolet 278.7, 285.0, 293.4 and 309.4 nm spectral ranges (Figure 13). In addition, well-known lines of Al I emission at 308.9 and 308.0 nm are important for phosphate rock analysis (Figure 14).

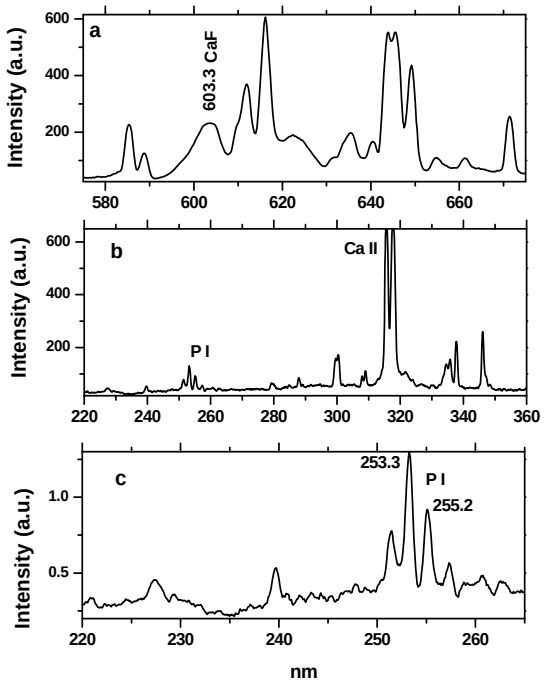

Figure 8. Double Pulse Breakdown Spectra of Apatite with P I, Ca II and CaF Emissions.

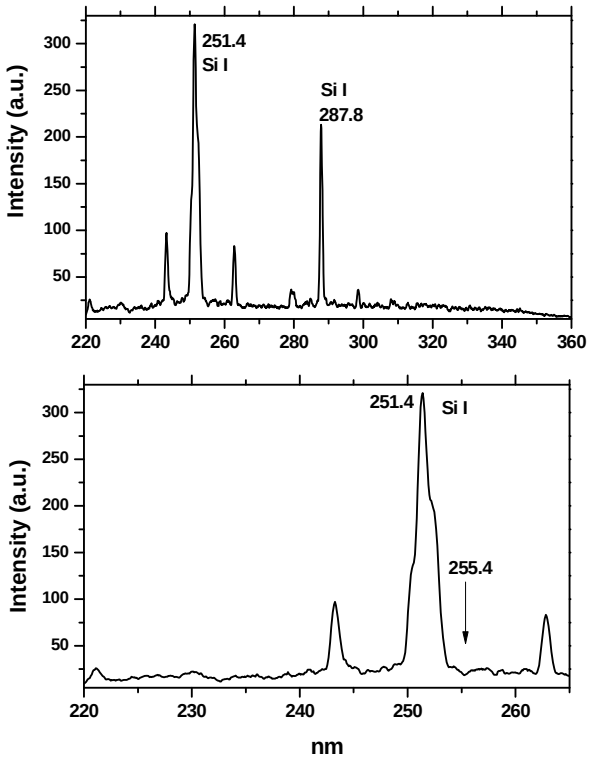

Figure 9. Double Pulse Breakdown Spectra of Quartz with Si I Emission.

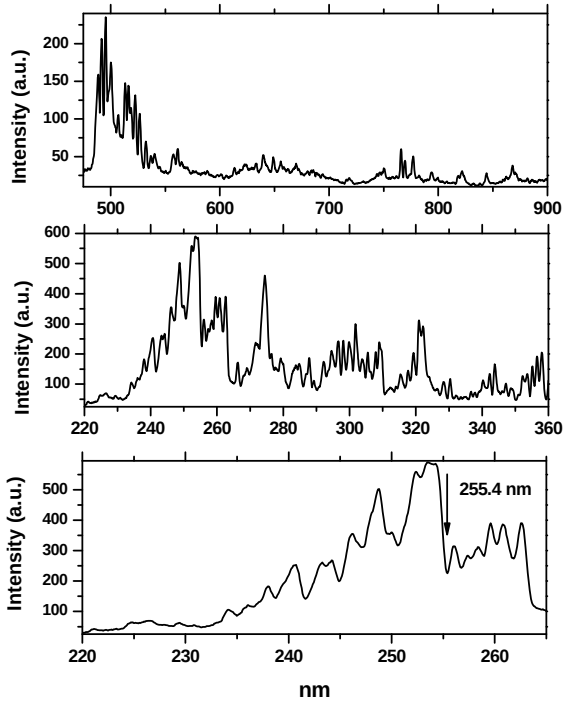

Figure 10. Double Pulse Breakdown Spectra of Hematite with Fe I and Fe II Emissions.

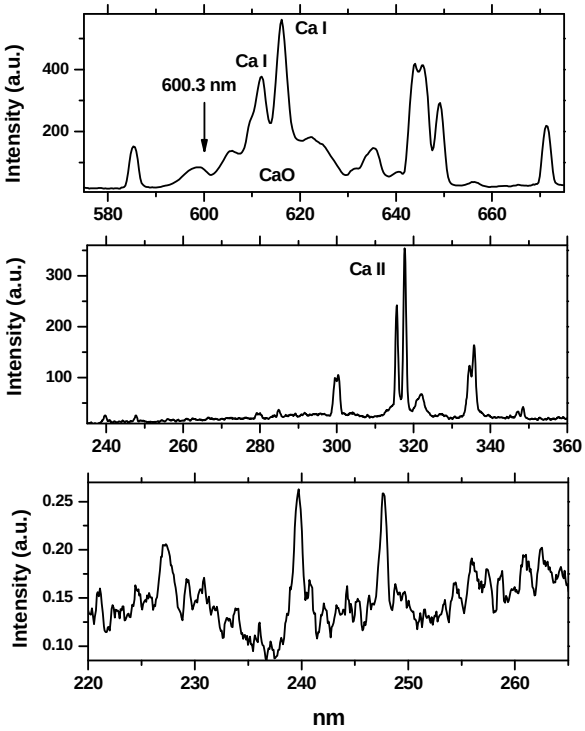

Figure 11. Double Pulse Breakdown Spectra of Calcite with Ca and CaO Emissions.

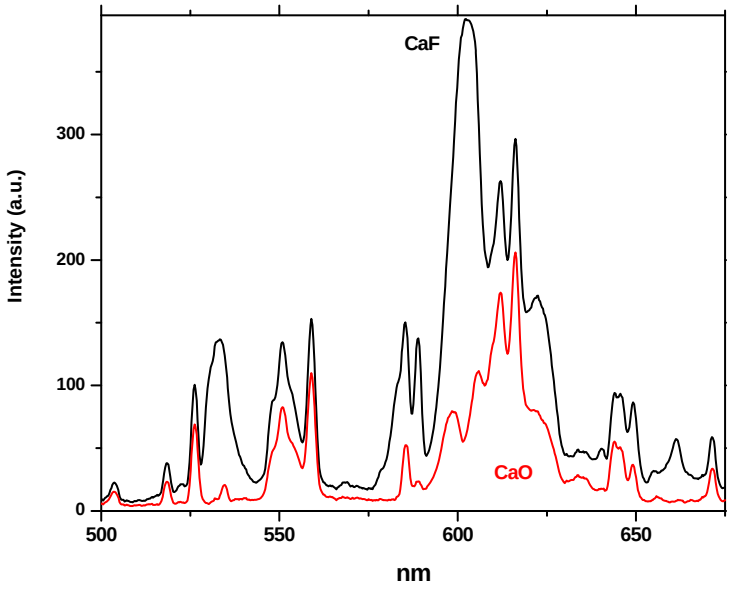

Figure 12. Double Pulse Breakdown Spectra of Apatite (black) and Calcite (red) with a Delay Time of 15 µs.

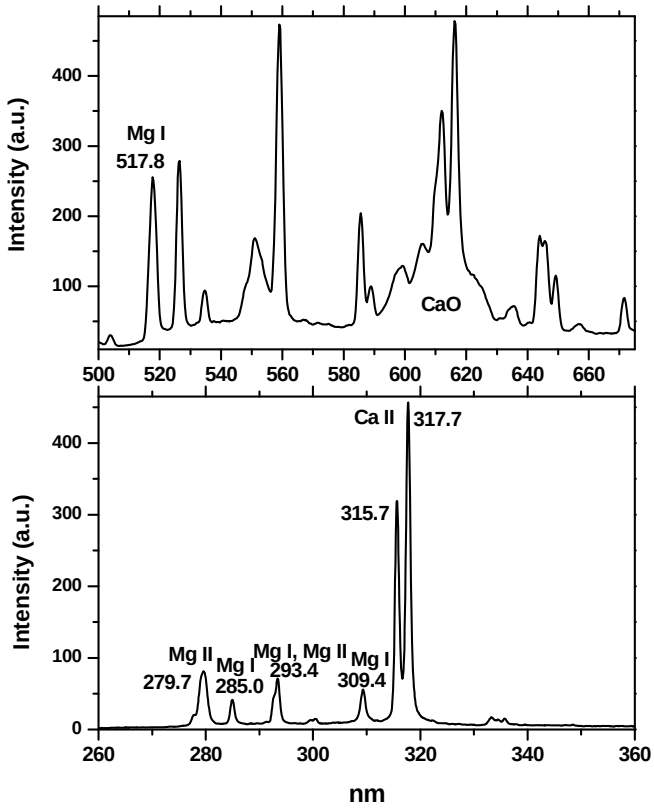

Figure 13. Double Pulse Breakdown Spectra of Dolomite with Mg Emissions.

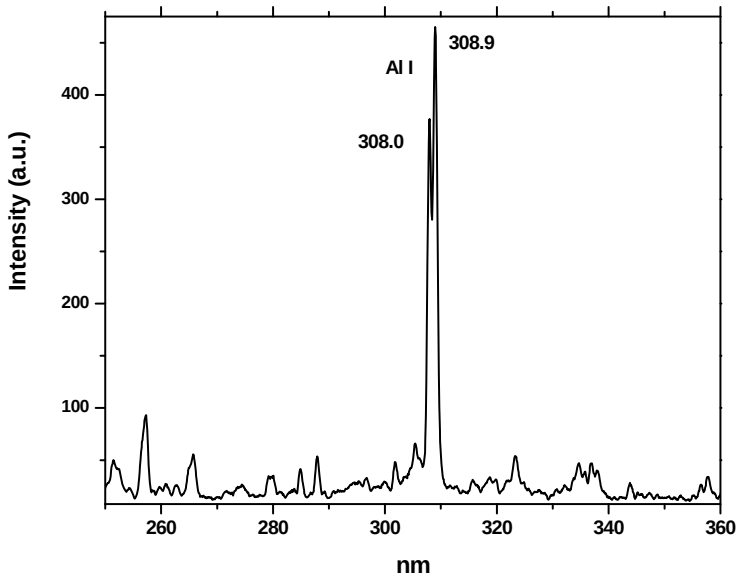

Figure 14. Double Pulse Breakdown Spectra of Corundum with Al I Emission.

Figure 15 demonstrates representative spectra received from Mosaic South Pasture rock samples (sample numbers and corresponding information are reported in Table 2). Because this is an ore and not pure minerals, the P_2O_5 concentrations are relatively low, while the acid insoluble portion, mainly quartz, is high. Thus in order to detect the P I emission lines more easily, the UV spectrometer was exchanged for one with a higher spectral resolution needed for the spectral separation of Si I and P I emission lines. It can be seen that all relevant elements, such as P, Mg, Ca, Si, Fe, Al and CaF, are definitely detected and reflects the ore compositions. For example, in sample N22, with a BPL of 27.0%, both P I lines and CaF bands are much stronger compared to the sample N7 with a BPL of 6.3%.

Table 2. Chemical Composition and Geological Description of Mosaic South Pasture Rock Samples.

N	BPL	Fe_2O_3	Al_2O_3	MgO	Insol	CaO	Company Description	Description Based on ReLIBS Analyses	
1	7.6	0.8	2.5	0.6	85.5	5.49	Overburden	Overburden	Mine?
2	5.1	0.2	3.4	0.2	87.0	2.0	Overburden	Overburden	Don't mine
3	17.6	10.	1.8	4.7	51.1	18.8	Bottom	Matrix	Mine?
7	6.3	1.00	1.6	0.9	84.1	4.7	Interburden	Interburden	Don't mine
8	24.4	1.30	2.7	1.1	61.5	17.3	Matrix	Matrix	Mine
9	24.9	0.73	1.0	2.6	54.4	20.4	Matrix	Matrix	Mine
10	3.2	0.3	2.2	0.1	92.4	0.4	Matrix	Overburden	Don't mine
11	5.0	3.1	2.3	0.9	83.6	3.4	Interburden	Interburden	Don't mine
12	21.6	1.1	1.6	1.5	62.6	16.0	Bottom	Matrix	Mine
13	0.3	0.1	0.1	0.0	97.4	0.2	Overburden	Overburden	Don't mine
14	3.6	0.5	0.5	0.1	92.9	2.3	Overburden	Overburden	Don't mine
21	0.3	0.1	0.2	0.1	97.7	0.3	Overburden	Overburden	Don't mine
22	27.0	1.2	1.4	0.3	59.8	18.4	Matrix	Matrix	Mine
23	11.6	1.1	1.8	2.2	69.7	10.3	Bottom	Matrix?	Mine?
24	2.7	0.3	1.1	0.1	92.6	1.4	Overburden	Overburden	Don't mine
25	9.9	1.3	2.0	5.6	56.5	13.8	Bottom	Bottom	Don't mine
26	18.3	1.1	1.5	4.9	49.9	18.6	Matrix	Matrix	Mine
27	18.9	1.1	1.7	3.9	51.3	17.7	Bottom	Matrix	Mine
28	6.2	1.2	2.1	0.8	80.9	4.1	Interburden	Interburden	Don't mine
29	22.9	1.1	2.1	0.5	64.5	15.3	Matrix	Matrix	Mine
30	0.3	0.1	0.2	0.1	97.7	0.3	Overburden	Overburden	Don't mine

During the previous stage of ReLIBS development and testing, spectral measurements were performed in the visible spectral range only. Thus the BPL was determined not by direct P I lines emission evaluation, but using CaO/Insol ratio. Now the BPL content can be measured both directly by the P I emission lines and CaF molecules emission bands. Figure 16 presents the results of remote LIBS analysis for the mostly important rock chemical composition components, such as BPL, Mg, Insol, and Fe. It may be seen that for all those elements the correlations between ReLIBS determined concentrations and the analytical data are reasonably good, with linearity coefficients (R^2) in the 0.9 range. BPL was determined by both the P I emission lines and CaF emission bands. Consequently, ReLIBS enables one to identify the matrix layers with high BPL content and further characterize them for high- and low-MgO segments.

Figure 17 presents representative spectra received by this experimental setup from the PCS Florida mine samples. The analytical lines of P, Mg, Ca, Si, Al, Fe, and CaF were easily detected and identified by our remote system from a 10 m distance. Figure 18 presents the preliminary results of remote LIBS analysis from a 10 m distance for PCS mine samples with different BPL contents. The most important element for online control in this case was Ca and it may be seen that the correlation of ReLIBS with the laboratory data ($R^2 = 0.8$) (Figure 18a) was quite reasonable and corresponded well with traditional online control of the conveyer LIBS analyzer from a distance of less than 0.5 m. In the PCS minerals, the main Ca-bearing mineral is apatite, and Ca is correlated with

the P content. The correlation is $R^2 = 0.83$ (Figure 18b). The correlation between P I lines and laboratory-determined concentrations were worse with $R^2 = 0.72$ (Figure 18c), which may be explained by the relatively low quality of breakdown spectra at the 250 nm range in this specific case, which is evidently connected with the fact that those samples were wet. It is important to note that the molecular CaF emission band is also well correlated with P laboratory data (Figure 17d, $R^2 = 0.82$), which makes it a potential tool for P online control in cases where other Ca-bearing minerals besides apatite are present, for example calcite.

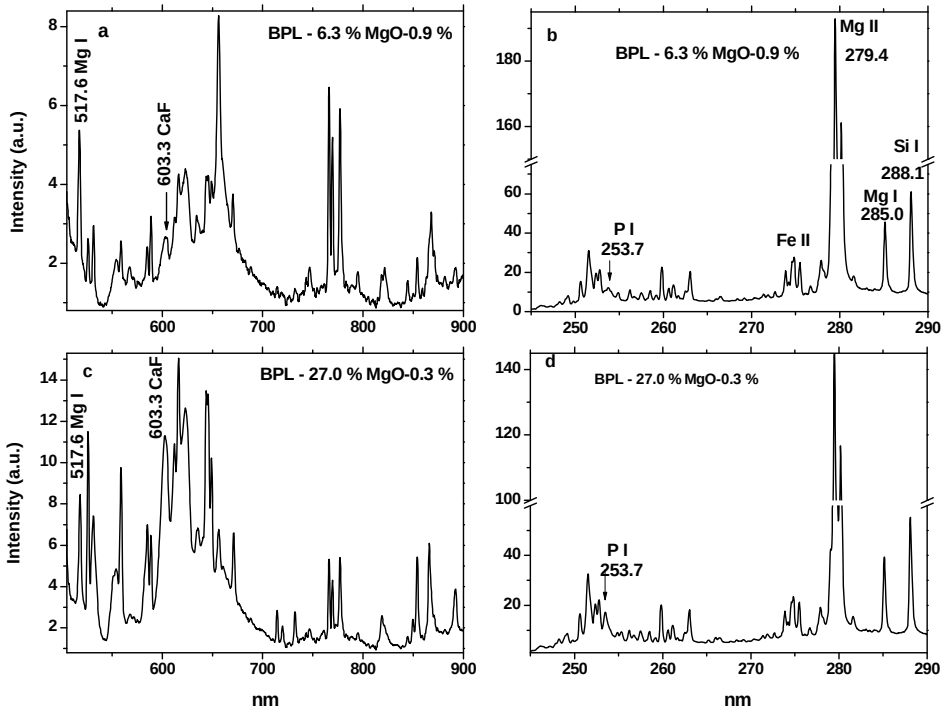

Figure 15. Representative Double Pulse Breakdown Spectra of Ores with Different BPL from Mosaic South Pasture Mine from 10 m Distance.

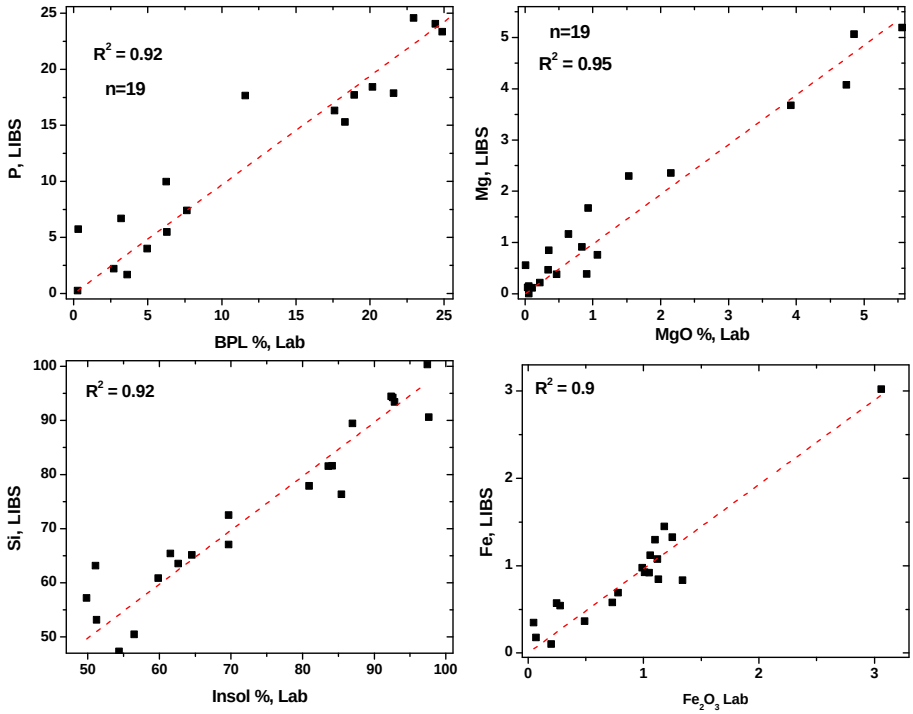

Figure 16. Calibration Curves of Different Elements for ReLIBS Analysis from 10 m Distance in Laboratory for Mosaic South Pasture Ores.

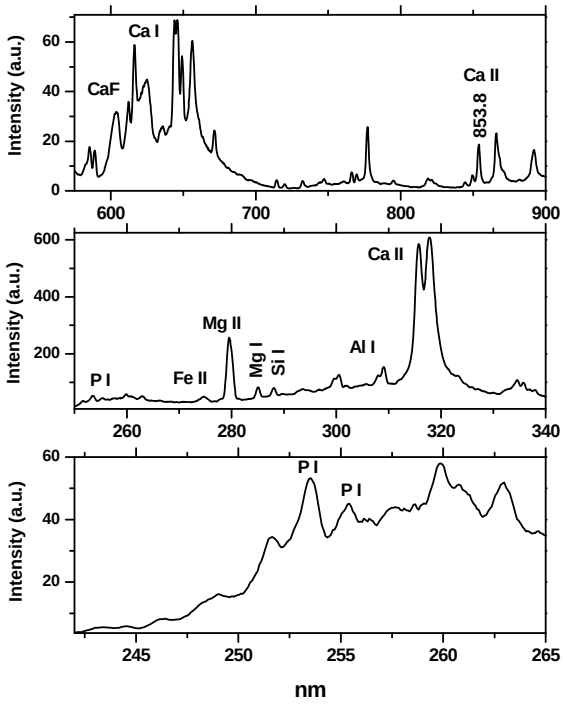

Figure 17. Double Pulse Breakdown Spectra of Phosphates from the PCS Mine from 10 m Distance.

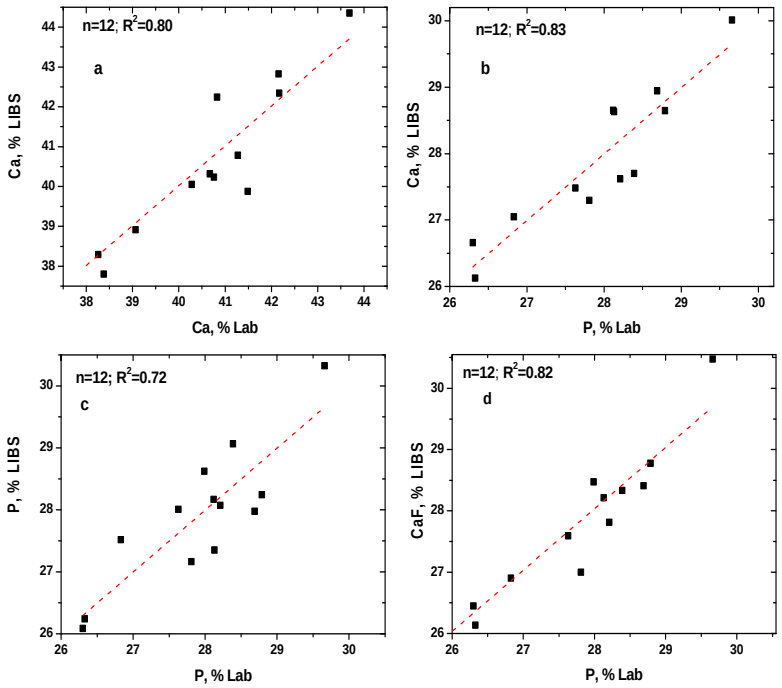

Figure 18. Calibration Curves of Different Elements for ReLIBS Analysis from 10 m Distance in Laboratory for the PCS Mine.

Figure 19 presents representative spectra received by the experimental setup using JDC (Florida) rock samples. The analytical lines of P, Mg, Ca, Si, Fe, and CaF were easily detected and identified by the remote system from a 10 m distance. Figure 21 presents the preliminary results of the remote LIBS analysis from a 10 m distance using the JDC mine samples. All relevant element concentrations determined by the laboratory correlate very well with the corresponding elements determined by ReLIBS from a 10 m distance. Both P I lines and CaF band emission intensity may be used for online BPL evaluation. A parameter of interest for the JDC industrial process is Si/(Ca+Mg) ratio. It may be seen that it may be determined based on the use of ReLIBS from a 10 m distance with a very high linearity coefficient $R^2 = 0.96$ (Fig. 20).

Figure 21 presents representative spectra received by this experimental setup using Xin Run (China) rock samples. The analytical lines of P, Mg, Ca, Si, Fe, and CaF are easily detected and identified by our remote system from a 10 m distance. Only the P_2O_5 concentrations were determined by laboratory analysis. Thus only the correlation between P_2O_5 with P I and CaF emission was studied. Figure 22 demonstrates that in both cases the correlation is very good with a linearity coefficient of $R^2 = 0.9$.

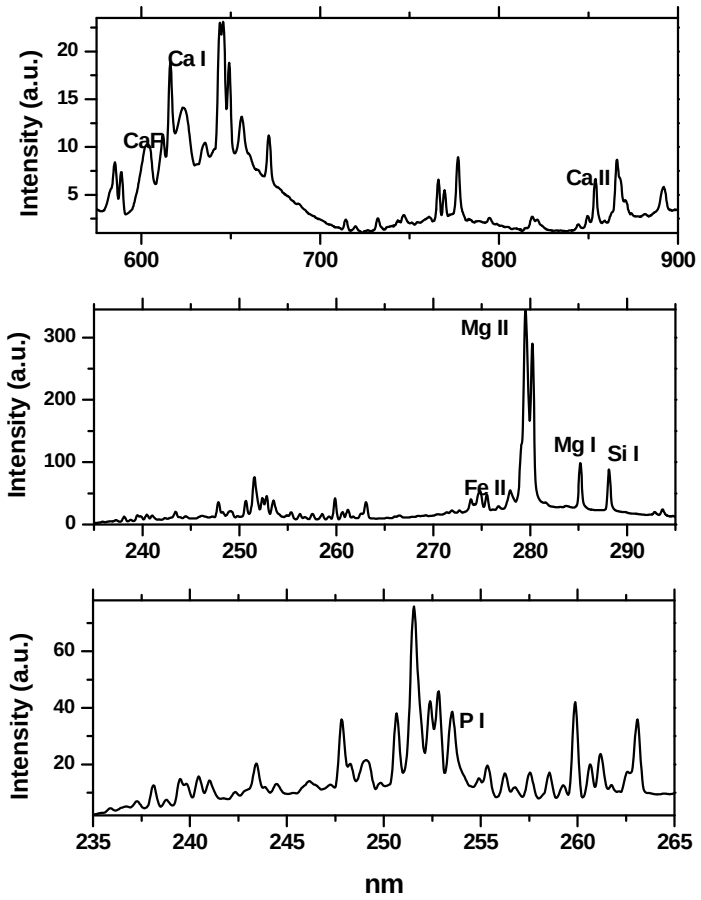

Figure 19. Double Pulse Breakdown Spectra of Phosphates from Samples from 10 m Distance.

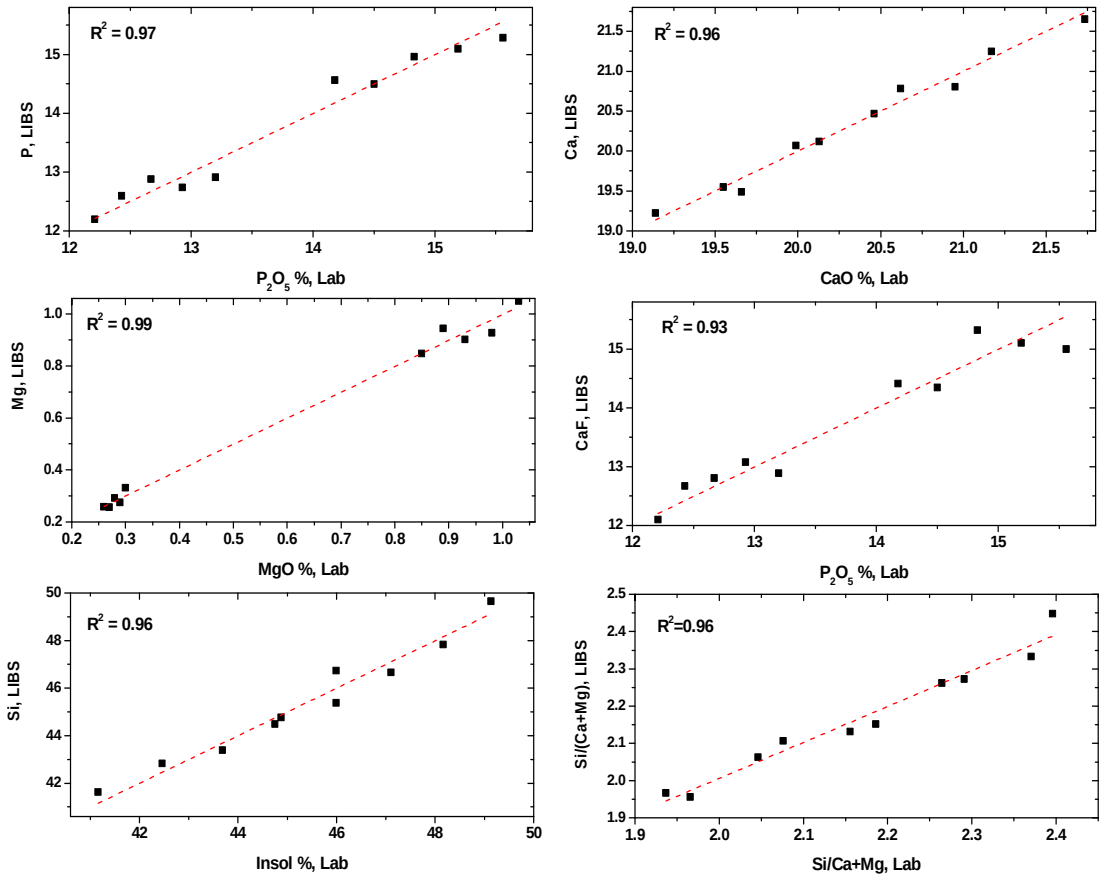

Figure 20. Calibration Curves of Different Elements for ReLIBS Analysis from 10 m Distance in Laboratory for JDC Samples.

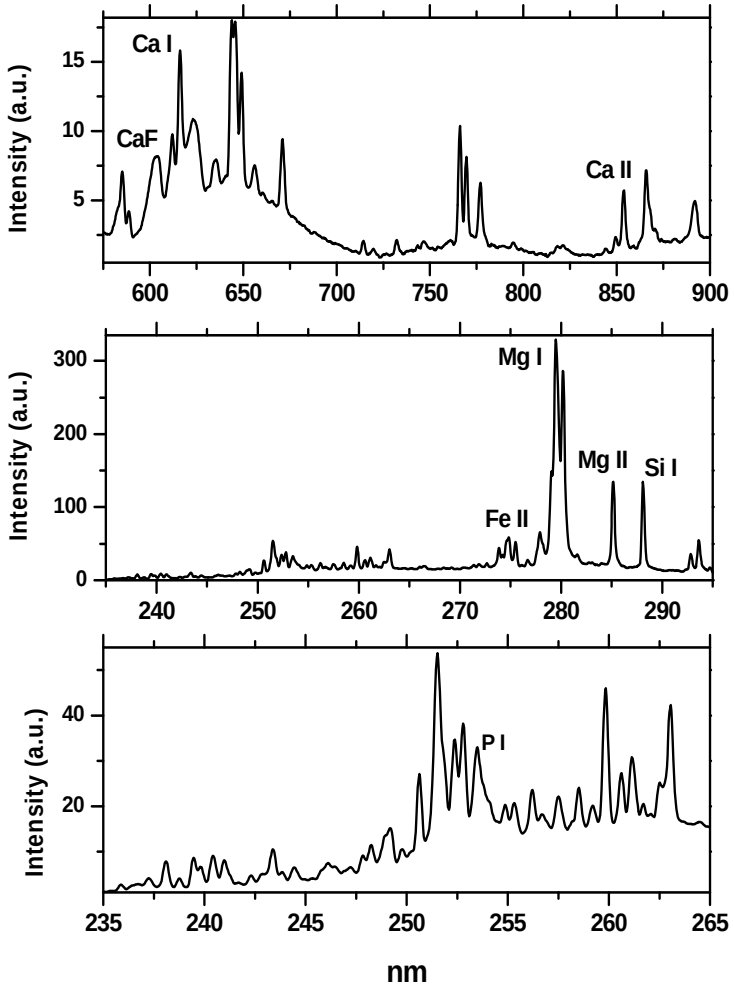

Figure 21. Double Pulse Breakdown Spectra of Phosphates from Xin Run Mine from 10 m Distance.

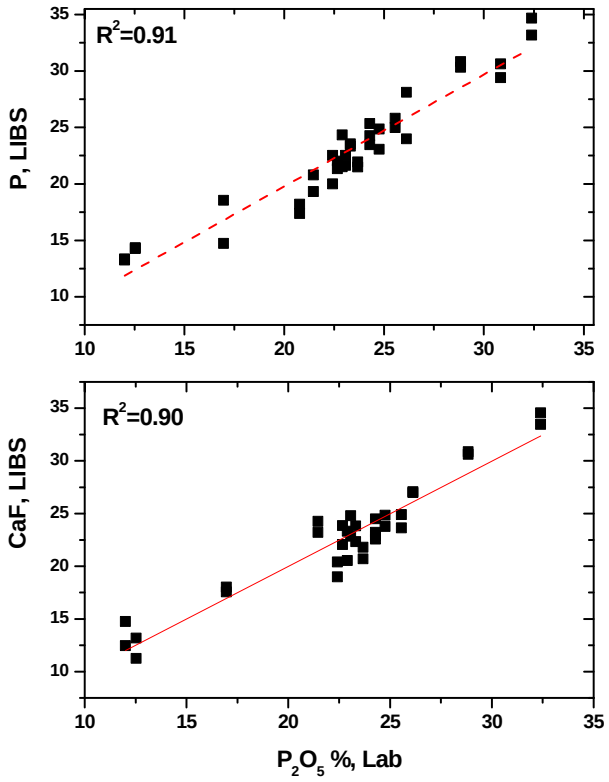

Figure 22. Calibration Curves of P_2O_5 for ReLIBS Analysis from 10 m Distance in Laboratory for Xin Run Mine.

ReLIBS from 20 m Distance – Ores from Mosaic South Pasture Deposit

Figure 23 presents typical breakdown spectra of phosphate rocks from Mosaic South Pasture ore measured from 20 m distance. The signals are approximately 4-5 times weaker compared to 10 m distance, which corresponds well to reciprocal distance relation between the signal intensity and the distance. UV spectrometers with both high and low spectral resolution were tested. It appears that the P I line is well detected by a high resolution spectrometer (Figure 23b), while it is not clearly detected by a low resolution spectrometer (Figure 23c). Other relevant elements, such as Ca, Mg, Si, Al, Fe, CaF are definitely found from this distance (Figures 23a-d). It was a good indication that quantitative evaluation is possible.

Figure 24 presents the results of remote LIBS analysis for the most important rock chemical composition components, such as BPL, Mg, Ca, Insol, and Fe. It may be seen that for all those elements the correlations between ReLIBS and analytical data are pretty good, with linearity coefficient in R^2 = 0.85-0.95 range. BPL was evaluated by both P I emission lines and CaF emission bands. Consequently, ReLIBS was able to identify matrix layers with high BPL contents and further evaluate them for high and low MgO segments.

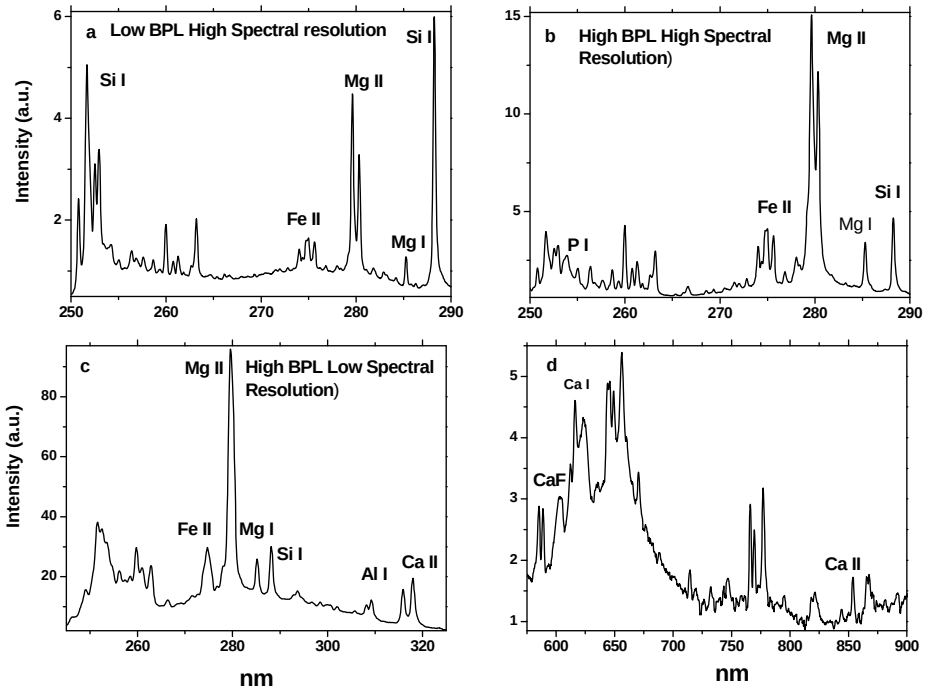

Figure 23. Double Pulse Breakdown Spectra of Phosphates from Mosaic South Pasture Mine from a 20 m Distance.

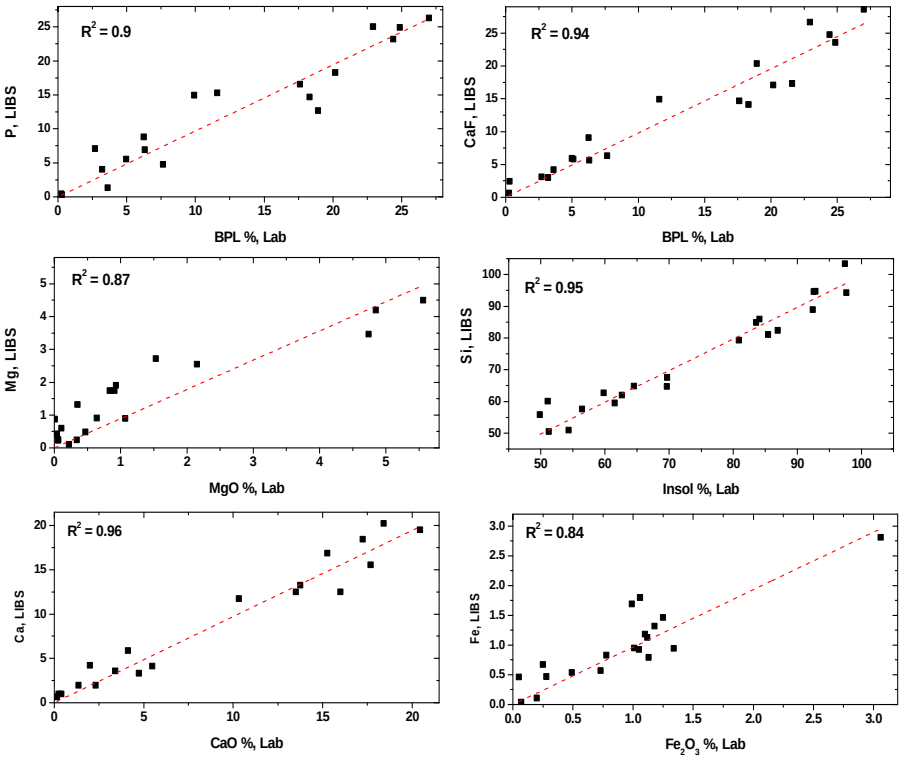

Figure 24. Calibration Curves of P_2O_5 for ReLIBS Analysis from 20 m Distance in the Laboratory for Mosaic South Pasture Mine.

FIELD EXPERIMENTS

The system was shipped to Florida with no damage and was assembled to working condition in four days. An important, and not expected, issue was the very high power voltage in the Mosaic plant due to the low level of industrial activity. The system was installed on a specially produced trailer and moved by truck (Figure 25).

Figure 25. Remote LIBS Unit During Transportation to the Test Site, Mosaic South Pasture Mine, Florida.

CALIBRATION ALGORITHM DEVELOPMENT

During the initial testing stage, the dragline operator (Figure 26a) put several piles of different ores, overburden, matrix and bottom, on the ground. Those piles were then subjected to analysis from distances of from 5-25 m using the ReLIBS unit (Figure 26b). It was found that plasma was created and detected by the remote unit from all the studied distances.

Figure 27 presents the typical breakdown spectra received from a 15 m distance of the sample visually determined as the good rock with the highest P_2O_5 content of 26.92% and MgO concentration of 1.26% according to the laboratory data. The most important analytical lines in the UV range are Ca, Mg, Si, Fe and Al (Figure 27a), while the main feature of the visible range is the relatively narrow bands peaking at approximately 603.0 nm, which is connected to the recently identified CaF emission. (It is interesting to note that using this band, the first detection of fluorine was made in Mars by the Curiosity mission.) In this spectrum the CaF band is a relatively strong, demonstrating high apatite, and correspondingly P_2O_5 content. At the other end of the spectrum, the Mg lines are relatively strong and the lines of Mg present at 293.1 nm, which usually only occurs at high Mg concentrations.

Figure 26a. Mosaic South Pasture Dragline Operation Site.

Figure 26b. Different Rock Piles Presented for the ReLIBS Test.

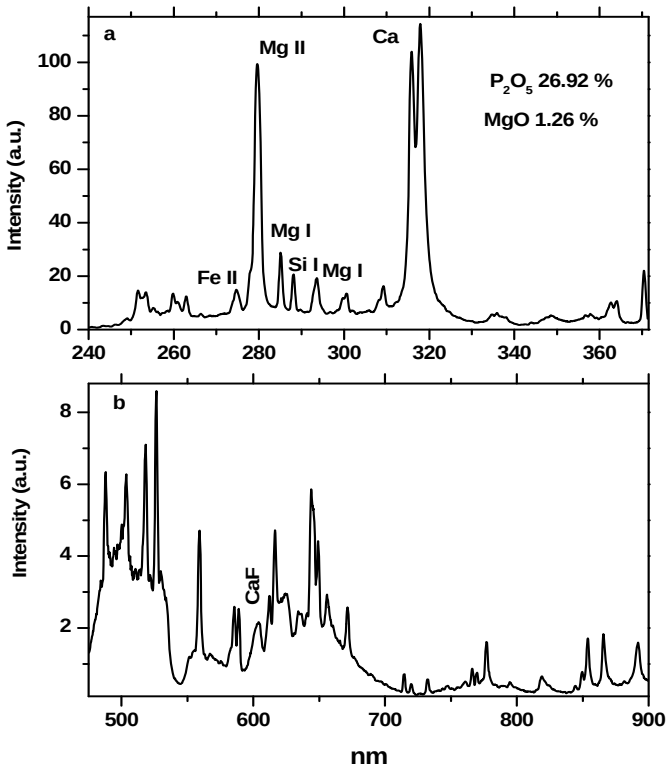

Figure 27. Typical Breakdown Spectra of the Rock with High P_2O_5 and Relatively Low MgO Content.

Figure 28 presents typical breakdown spectra received from a 15 m distance of the sample visually determined as waste material with a modest P_2O_5 content of 15.28% and very high MgO concentration of 7.0%, according to the laboratory data. Correspondingly, the CaF band is still detected, while the Mg lines are substantially stronger, including the emission at 293 nm. With such a high MgO content, the so-called concentration quenching already is taking place and the resonance Mg emission lines in the UV range are not the best for analytical applications. In such a case, the non-resonance Mg I line at 518.0 nm is a preferential one and its relative dominance is easily seen in this sample.

Figure 29 presents typical breakdown spectra received from a 15 m distance of the sample visually determined as upper zone with a modest P_2O_5 content of 14.03% and very low MgO concentration of 0.31%, as determined by the laboratory data. Correspondingly, the CaF band is still detected but in much weaker fashion compared to the previous samples, while the Mg lines are substantially weaker, including the absence of emission at 293 nm.

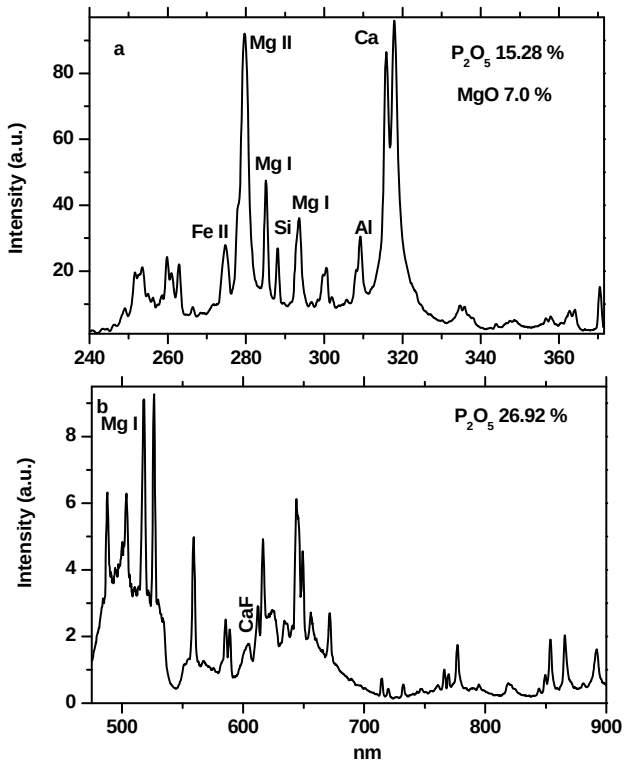

Figure 28. Typical Breakdown Spectra of the Rock with High P_2O_5 and Very High MgO Content.

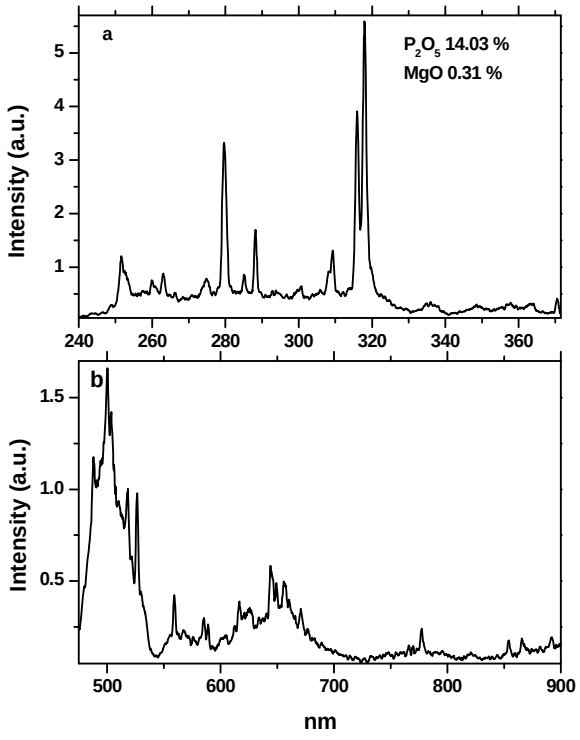

Figure 29. Typical Breakdown Spectra of the Rock with Relatively High P_2O_5 and Low MgO Content.

Figure 30 presents a typical breakdown spectra observed from a 15 m distance from the sample that was visually determined to be overburden with a very low P_2O_5 content of 0.56% and very low MgO concentration of 0.08%, as determined by the laboratory data. In addition, the CaO content is also very low at 0.54 %. In such a case, the visible spectrum has very low intensity spectra. In the UV spectrum, Fe, Si and Al dominate.

The next step was to evaluate the ability for quantitative chemical analysis of all relevant elements. All remotely analyzed ores, 16 total, were sampled and sent to the Mosaic laboratory (Table 3) for routine analysis in order to get the calibration curves for all relevant elements, such as P, Mg, Fe, Al, Si, Ca, and F. Figure 31 presents the corresponding calibration curve for P_2O_5, which is one of the most important elements. The linearity coefficient $R^2 = 0.91$ is very good for real-time process control. Another important task is remote evaluation of the MgO content. Figure 32 presents the corresponding correlation between ReLIBS and laboratory data, demonstrating very good linearity coefficient of 0.98. Thus it may be concluded that remote LIBS is a promising tool for real-time analyses of the phosphate materials excavated by the draglines. The linearity coefficient of 0.91 for CaO is also very good, while for SiO_2 vs. Acid Insol (AI) it is approximately 0.73, which is usually the border value for real-time process control (Figure 33).

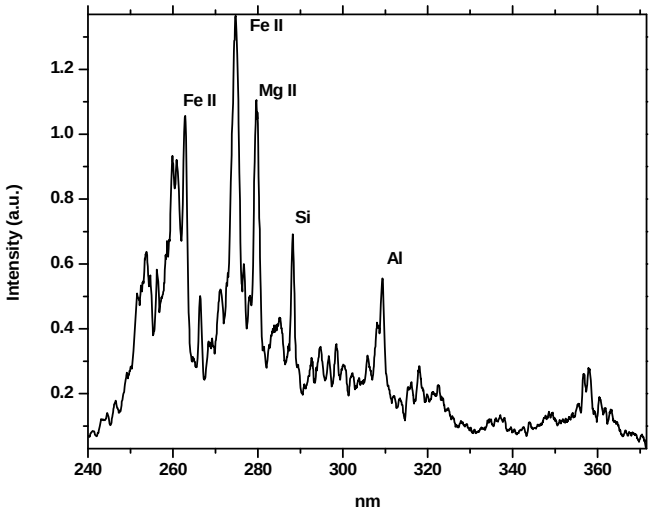

Figure 30. Typical Breakdown Spectra of the Rock with Relatively Very Low P_2O_5, MgO and CaO Content.

The autofocus system effectiveness and, correspondingly, plasma creation and its emission detection depend strongly on the distance measuring accuracy. The ability to both create strong plasma and measure the spectral intensity is a strong function of the degree of focus obtained. It has to be noted that the materials tested represent one of the worst possible scenarios. They are usually crumbly, wet, with grey-black colors which are characterized by a low reflection ability. Contrary to this, solid targets, such as pebbles, bones, vertebrates have much higher reflection coefficients and are characterized by much stronger plasma emission signals. For example, Figures 34 a-b present the

breakdown spectra of a big vertebrate and fish bone measured from 12.5 m distance in the visible range, where the detected signal is relatively weak compared to the UV spectral range. The bone spectrum was measured at larger distances up to 21.5 m (Figures 34 c-d). The detected signals intensity is lower, but the spectral type remains the same.

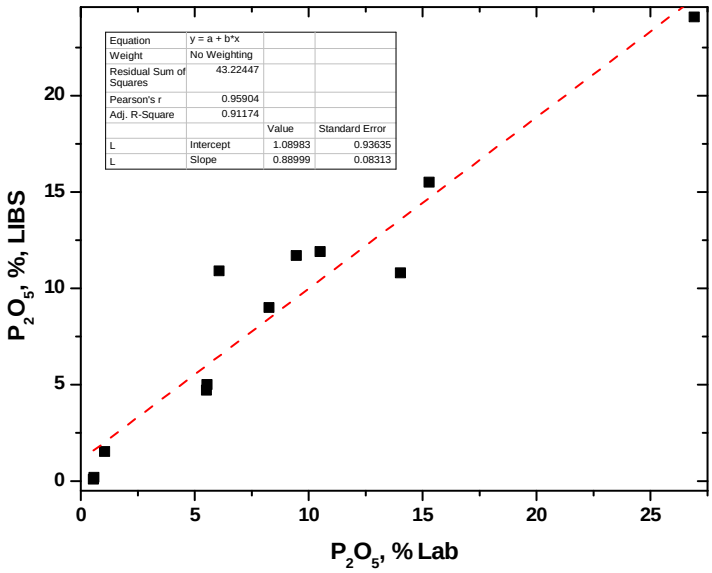

Figure 31. Correlation Between ReLIBS and Laboratory Data for P_2O_5.

Table 3. Laboratory Analytical Data for 16 Rock Samples Selected for Calibration Curve Development.

P_2O_5	Fe_2O_3	Al_2O_3	MgO	CaO	SiO_2	F	C	A.I.
17.44	1.89	3.81	0.6	25.87	4.46	1.81	2.32	41.29
5.84	0.86	1.18	9.77	23.39	1.81	0.55	2.45	32.58
13.92	1.35	1.19	0.58	20.93	2.51	1.57	2.34	54.85
6.88	0.67	0.85	8.7	22.56	1.6	0.69	2.26	35.52
5.54	0.93	1.4	8.82	21.48	1.97	0.56		37.77
10.5	0.77	3.94	0.41	15.23	3.38	1.1		62.99
14.03	0.96	3.64	0.31	20.52	3.66	1.41		53.79
9.45	0.44	4.24	0.19	13.08	3.64	0.89		66.95
1.04	0.14	0.55	0.08	1.62	0.58	0.18		92.25
5.52	0.91	2.17	0.69	8.37	1.93	0.5		74.91
6.07	0.85	2.1	0.63	9.22	2.38	0.71		74.64
8.26	1.02	2.62	0.63	12.46	2.69	0.78		69.21
0.56	1.5	1.09	0.08	0.54	0.86	0.1		93.15
0.58	1.63	1.01	0.09	0.66	0.77	0.1		92.33
15.28	2.18	1.15	7	33.56	2.33	1.66		16.06
26.92	2.15	1.13	1.26	41.55	2.33	2.84		12.33

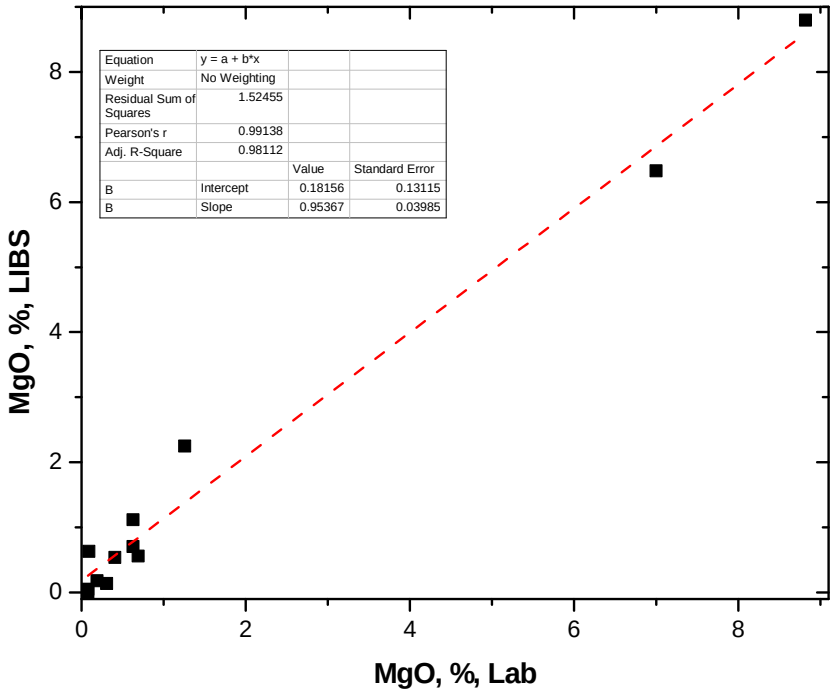

Figure 32. Correlation Between ReLIBS and Laboratory Data for MgO.

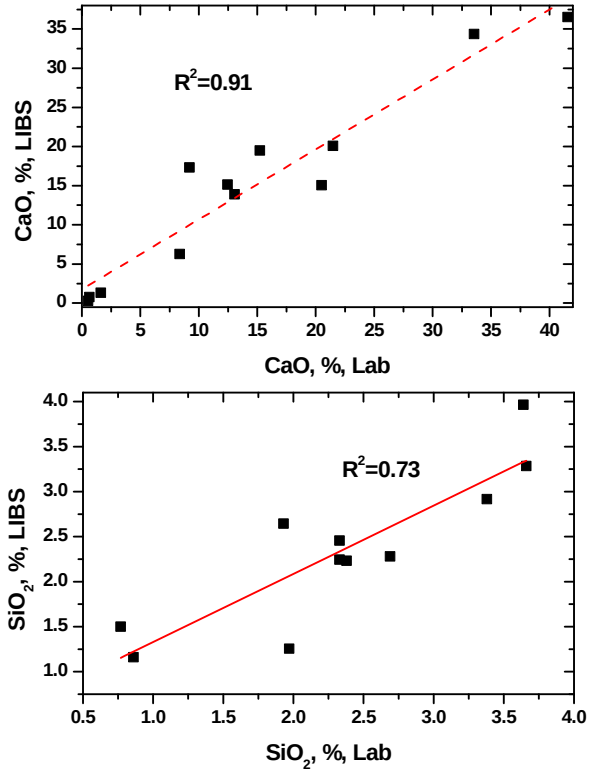

Figure 33. Correlation Between ReLIBS and Laboratory Data for (a) CaO and (b) SiO_2.

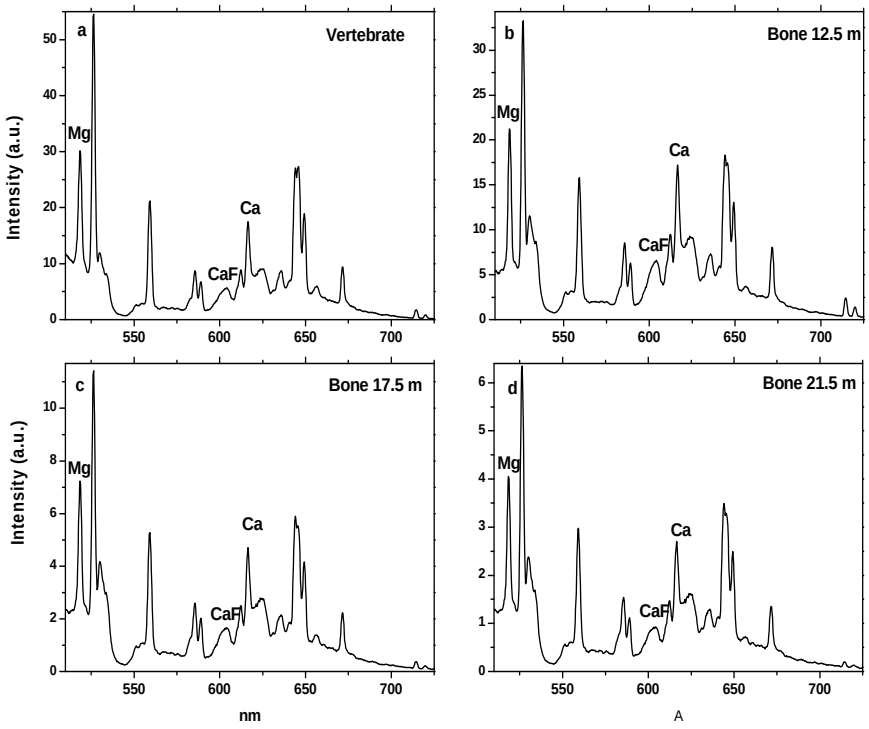

Figure 34. Breakdown Spectra of Vertebrate and Bone in the Visible Range.

In this system, the UV spectrometer is much more sensitive than the visible one (Figure 35). UV plasma emission spectra from, for example, bone have been easily measured at distances of 25-26 m, which is the limit for the present system. Good spectra were measured at a distance of 17.5 m not only for bone (Figure 35a), but also for pebble inside the matrix (Figure 35b), matrix (Figure 35c) and even strongly wet matrix (Figure 35d).

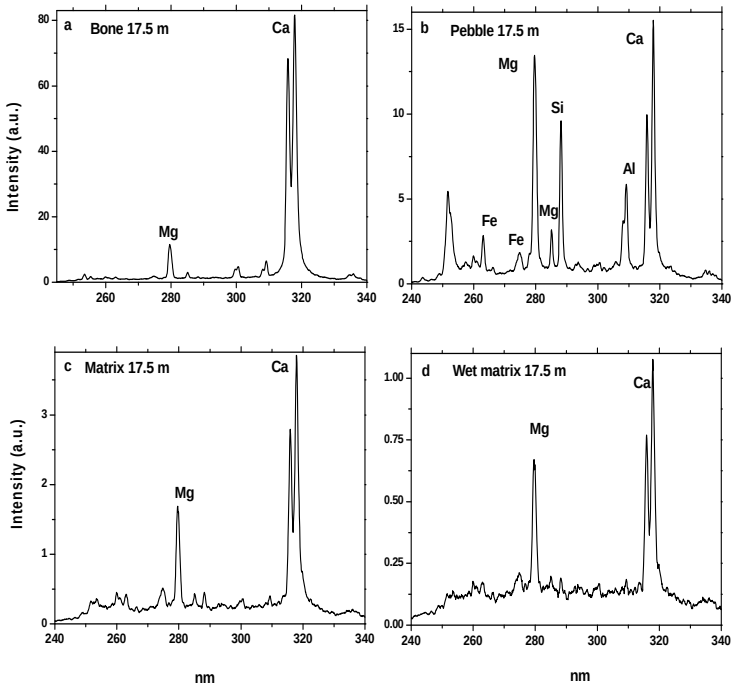

Figure 35. Breakdown Spectra of Bone and Matrix in the UV Range.

Figure 36a presents breakdown spectra of a bone detected from 18 m distance using a spectrometer with a high spectral resolution. It may be seen that two characteristic P emission lines may be confidently detected. In this case with a very high P_2O_5 content and low Fe impurities, the P lines are very clear. In the pebble fraction of the matrix, where P_2O_5 content is lower and the concentration of Fe impurities is higher, only the strongest P emission line may be seen, and not in its clear form (Figure 36b). It looks broader because of the spectral interference of Fe emission lines, which may not be prevented even with this high spectral resolution.

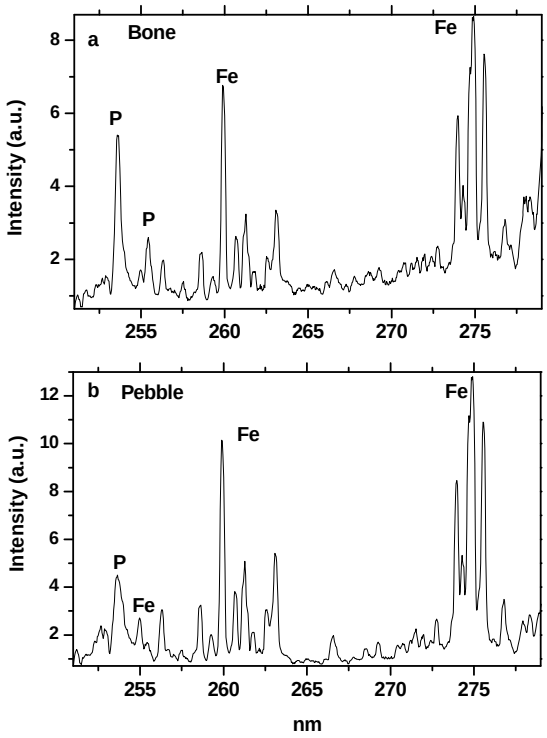

Figure 36. Breakdown Spectra of Bone and Pebble in the UV Range with High Spectral Resolution Enabling P Emission Line Detection.

SELECTION OF THE BEST IMPLEMENTATION SITE

The main task of ReLIBS is to use this analyzer for "horizon control" in open mining. Phosphate rock is usually found 15-50 feet beneath the ground in a mixture of phosphate pebbles, sand and clay known as phosphate "matrix." The sandy layer above the matrix, called the overburden, is removed using electrically operated draglines. Equipped with large buckets, these draglines remove the overburden, placing it in the previously mined voids, and excavate the matrix, depositing it into a shallow containment area or slurry pit. There, high-pressure water guns turn the material into a watery mixture called slurry, which is sent through pipelines to a processing facility, where phosphate rock is physically separated from the sand and clay in the matrix.

Presently the dragline operators are advised by field geologists on what to mine based on information from drill cores and visual observation. Nevertheless, such information may be erroneous. This generally results in at least some inclusion of overburden or base material in with the phosphate matrix or matrix is cast aside with the overburden or left it in the mine cut. For example, in one of the tests, 56 samples of "Overburden," "Matrix," and "Bed," according to the dragline operator practice were collected from 7 mines and analyzed. Out of the 51 samples which were clearly "Mine" or "No Mine," only 75% were correct. Compared to what was actually being mined, "correct" mining would have increased production by 9% and reduced MgO by 50%, but

actual mining was being controlled by the dragline operators. What if a geologist had been present? The same 56 samples were viewed by five geologists and characterized as to "Mine" or "No Mine." Average accuracy was 79% (73-84%). All five got the right answer on 31 of the samples and the wrong answer on 3 of the samples. Both the dragline operators and geologists were mining "Matrix" containing as low as 2% BPL or with an MgO over 8%. Both the dragline operators and geologists were leaving overburden or bed containing over 30% BPL and less than 0.2% MgO. It is not always possible to "see" the difference between matrix and non-matrix and chemical analysis is required to make the correct determination. At one mine, samples of overburden, matrix and bed at each dragline were taken each day. Several hundred samples were taken. Depending on the criteria used for "good rock," the accuracy of what was being mined (compared to what should have been mined) was 70-85%.

The impact of "correct mining" will be to increase both production and improve mined rock quality. But where is the best place to locate the ReLIBS unit? As a result of the previous ReLIBS field test, the washing pit was selected, which is where the dragline operator places the excavated matrix for its transformation to slurry and the subsequent pumping to the beneficiation plant (Figure 37). The advantages of this position are the following:

- The information for the dragline operator is practically real-time, only one bucket later compared to information from a unit mounted on the dragline machine being the fastest.
- Not every bucket has to be controlled, but only those in the unclear excavating zones.
- The distance from the ReLIBS to the pit can be approximately 15-20 m, which is in the range of existing capabilities.
- The relief is substantially less changeable compared to the actual surface.
- The safety issue is substantially less severe because there are no personnel present in this area.

A potential problem may be the slowing down of the sluicing process, because it may have to be stopped for a certain time to accomplish the scanning process. However, this was not the case as the proper collaboration of activity between the dragline and water-guns operators and the ReLIBS analysis was performed without slowing down the sluicing process. Based on field observations, there is adequate time for the ReLIBS scanning before the rock is washed into the pit.

CRITERIA FOR ROCK REMOTE IDENTIFICATION

For safety reasons, it was not possible to take actual pit field samples for laboratory analysis to correlate with the specific ReLIBS samples. Thus we selected the spectral types based on different emission lines relative intensities as an indicator of the rock types. In order to do this, the spectra of the rock samples, previously analyzed by the Mosaic laboratory, were measured under laboratory conditions. Figure 38 presents

the total spectra of those samples in UV spectral range. As it was found in our previous studies of the Florida phosphate rocks, the mostly important elements are Ca, Mg, Si, Al, Fe. Calcium is mainly contained in apatite, while magnesium is in dolomite and their ratio is a good indication of apatite/dolomite ratio in the rocks. Silicon, iron and aluminum are mainly contained in sand and clays. Additionally, Ti impurities have been found in certain samples.

Figure 37. ReLIBS Unit Situated at Washing Pit Site Facing Matrix Rock Delivered by the Dragline.

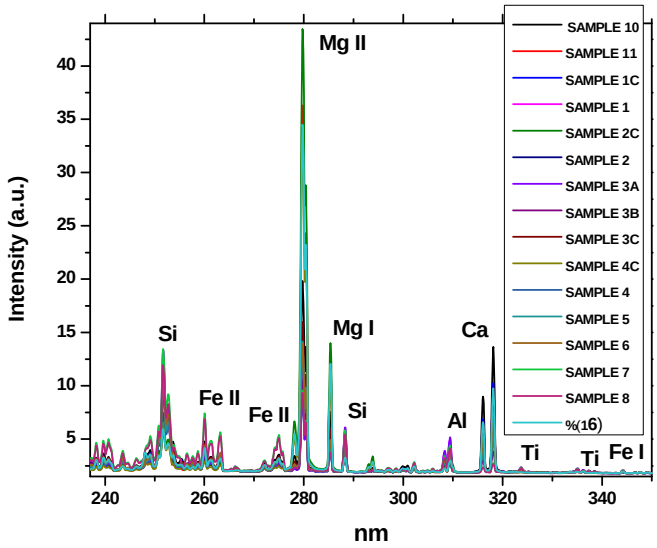

Figure 38. Breakdown UV Spectra of the Analyzed Different Rock Samples Measured by DP LIBS in Laboratory.

As was previously mentioned, in this study both UV and visible spectral ranges were utilized, where the main new feature was CaF molecular emission peaking at approximately 603 nm (Figure 39). Because fluorine is definitely contained in the apatite only, the CaF emission presents a direct and not oblique analytical feature for quantifying apatite, and consequently P_2O_5, measurement. It was demonstrated by a very good correlation between the CaF molecular emission intensity and measured P_2O_5 concentrations determined in the Mosaic laboratory with an $R^2 = 0.95$ (Figure 40). In addition, molecular CaO emission is detected together with Ca, Mg, Na and K atomic emission lines.

While an emission line of P also may be seen with high resolution spectrometry in the UV range of 245-260 nm (Figure 41), P_2O_5 concentrations evaluated based on its emission lines demonstrate a lower correlation linear coefficient of $R^2 = 0.91$ (Figure 42). The reason is that there are many intensive emission lines of Fe present in this spectral region that interfere with the measurement of the P emission. Because of this interference, one sample was omitted in the calibration process because the P lines were not be seen due to the Fe emission background.

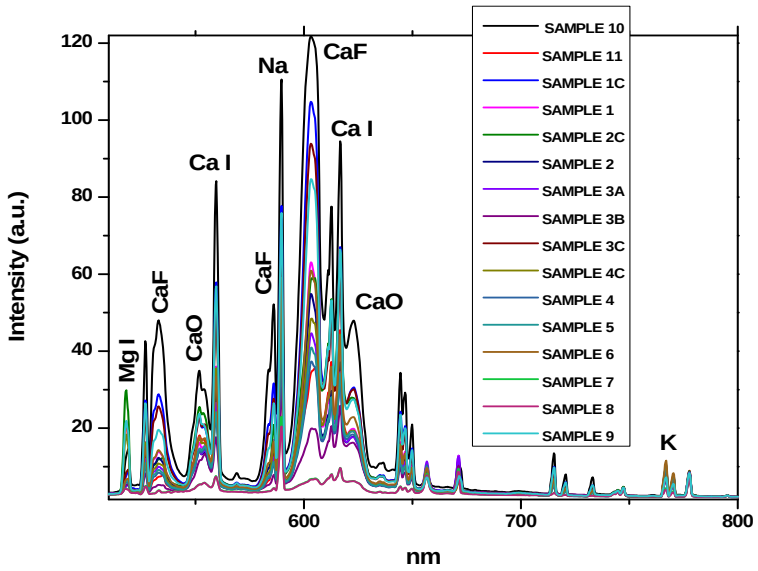

Figure 39. Breakdown Visible Spectra of the Analyzed Different Rock Samples Measured by DP LIBS in the Laboratory.

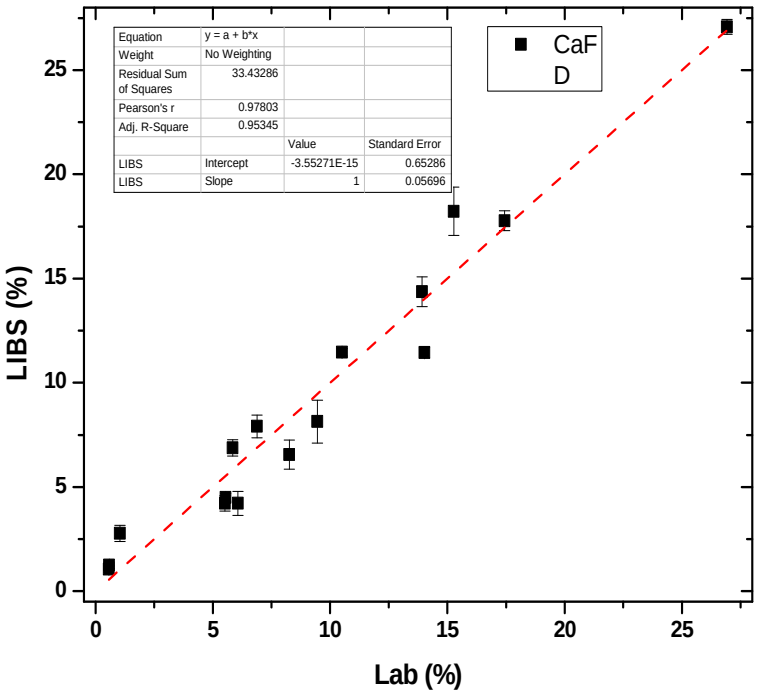

Figure 40. Correlation Between Laboratory-Determined P_2O_5 and That Evaluated Based on Intensity of CaF Emission in Breakdown Spectra.

Because of this interference, one sample was omitted in the calibration process because P lines were not seen due to the Fe emission background.

Thus it may be concluded, that CaF emission is the best indication of high apatite presence, while Mg is a definite dolomite signature and Si, Fe and Al are mostly sand and clay constituents.

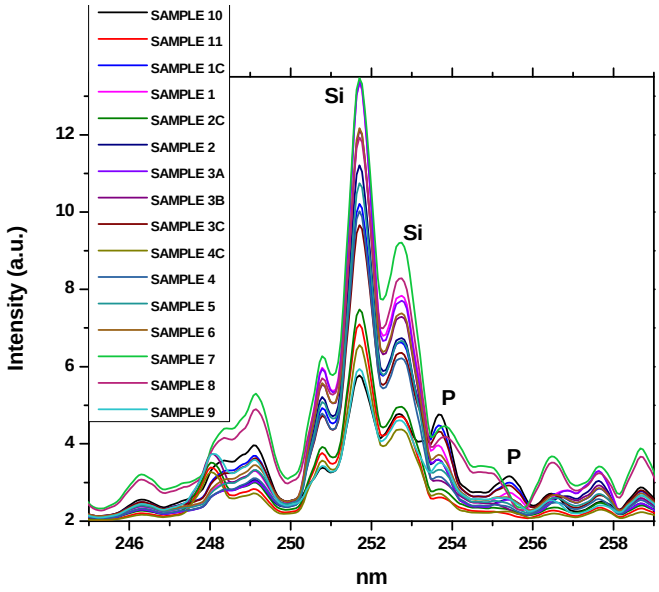

Figure 41. Breakdown High Spectral Resolution UV Spectra of the Analyzed Different Rock Samples Measured by DP LIBS in Laboratory.

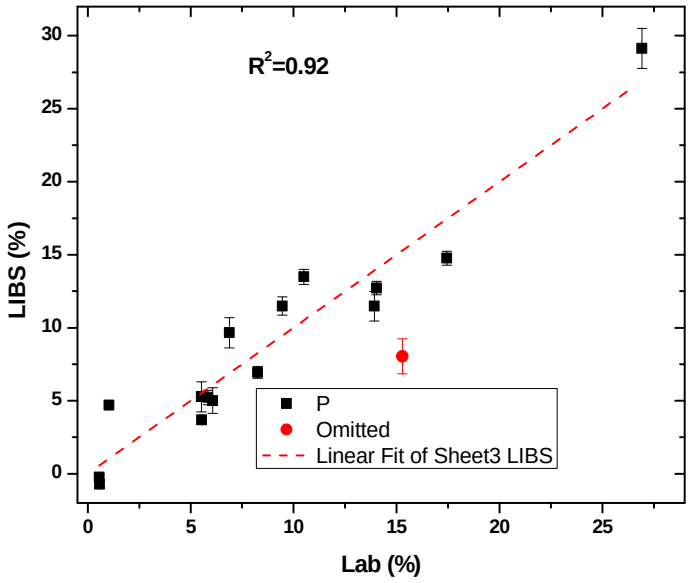

Figure 42. Correlation Between Laboratory-Determined P_2O_5 and That Evaluated Based on Intensity of P Line Emission in Breakdown Spectra.

EXPERIMENTAL RESULTS

Several types of spectra were detected during the field testing at the washing pit. In the first spectrum, magnesium and calcium lines were mainly detected in the UV part of the spectrum (Figure 43a) in the light gray type of rock (Figure 44). The lines of Mg were very strong and dominated the spectrum. Even Mg II lines peaking at

approximately 293 nm were clearly detected, which is a sure sign of very high Mg concentration, indicating high dolomite. High Mg presence is confirmed by a relatively strong line peaking at approximately 518 nm in the visible part of the spectrum (Figure 43b). This line is the best indicator for Mg measurement when its concentration is very high. The reason is that this line is not resonant and to a lesser extent is subjected to concentration quenching compared to the UV emission lines. The CaF band of apatite is also seen in the visible part of the spectrum, but its relative intensity is extremely low.

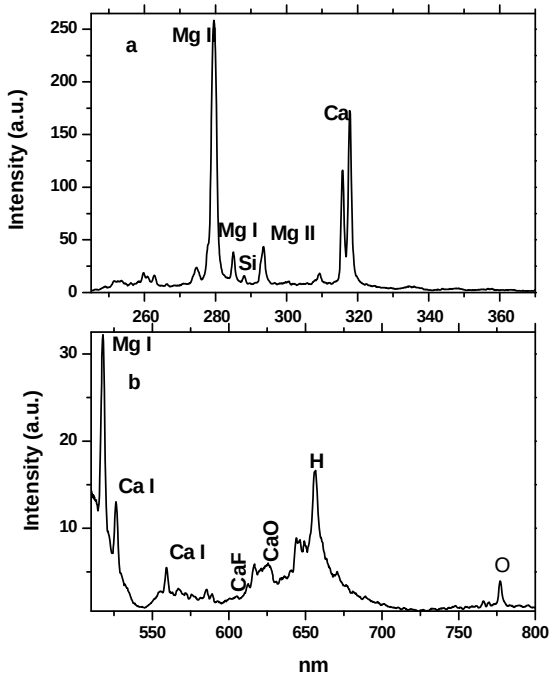

Figure 43. Breakdown Spectra with Very Strong Mg Lines and Evidently High Dolomite Content.

Figure 44. Material with Breakdown Spectrum from Figure 43.

In the second rock type, the Ca/Mg ratio was much higher, indicating a lower dolomite concentration (Figure 45a). The CaF emission may be seen but its relative intensity is still low enough (Figure 45b). The picture of this specific rock type is presented by Figure 46. Figure 47 shows the spectrum from a "very good" matrix. Calcium emission lines totally dominated the UV spectrum, with only very weak lines of Mg, Si and Al. High apatite content is further confirmed by the relatively strong CaF emission band in the visible part of the spectrum. Figure 48 presents the picture of the corresponding rock. Figure 49 presents an unusual spectrum where a high Ca/Mg emission line ratio and strong CaF band emission were accompanied by strong emission lines of Fe. This would indicate a matrix that is rich in phosphate but also contains high iron. This could also indicate a contact zone with two types of rocks. Figure 50 presents the picture of the corresponding rock. Figure 51 presents spectra typical for the host clay bearing ore, characterized by weak to very weak Ca emission lines and relatively strong lines of Si, Fe, Al and Mg.

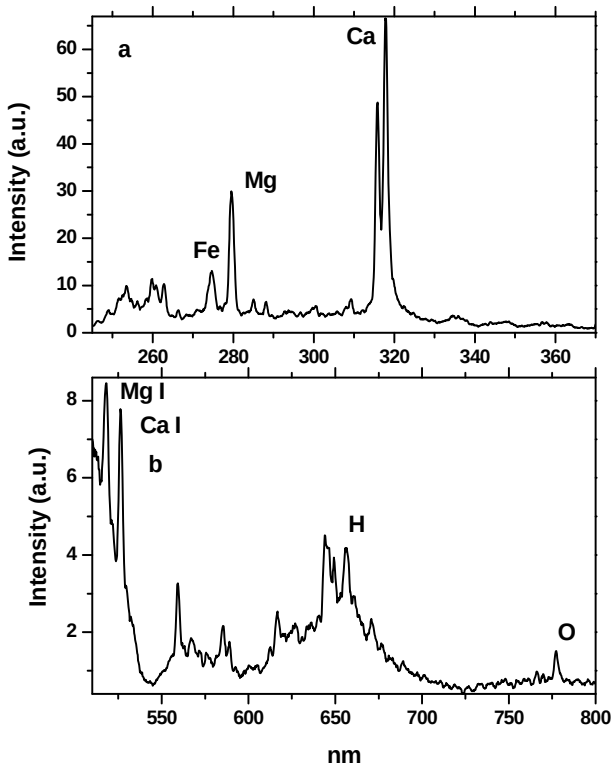

Figure 45. Breakdown Spectra with High Ca/Mg Lines Ratio and Evidently Relatively Low Dolomite Content.

Figure 46. Material with Breakdown Spectrum from Figure 45.

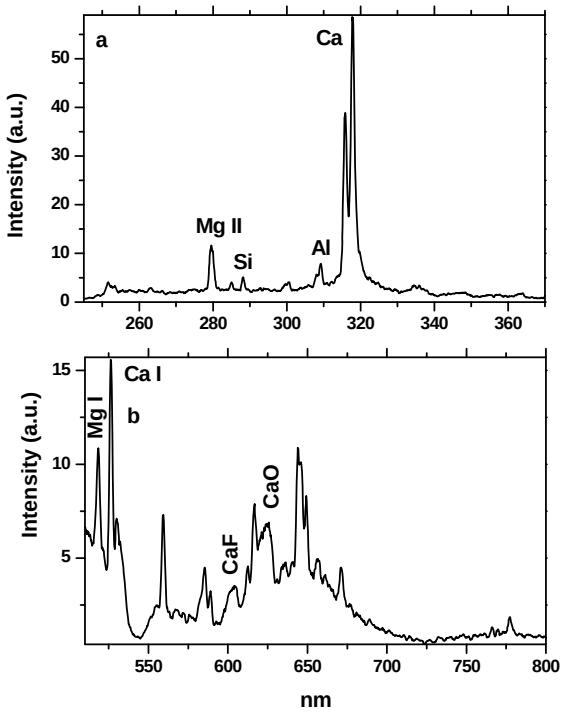

Figure 47. Breakdown Spectra with Very High Ca/Mg Lines Ratio and Strong Band of CaF Emission Evidencing Very High Apatite Presence.

Figure 48. Material with Breakdown Spectrum from Figure 47.

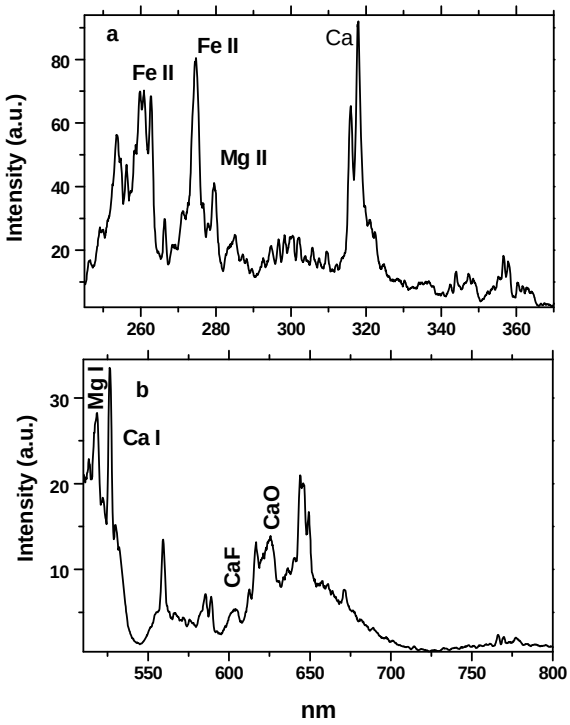

Figure 49. Breakdown Spectra with High Ca/Mg Ratio and Strong CaF Emission Evidencing High Apatite and Fe Presence.

Figure 50. Material with Breakdown Spectrum from Figure 49.

Based on calibration curves developed from the calibration sample (Table 3), spectroscopic data can be interpreted to give the chemical compositions. The corresponding results are presented in Table 4. Based on all the information, it appears that 5 of the 24 presented samples represent material that should not have been mined as it would supply rock of low value to the chemical plant. This is similar to the results reported previously in 1997 when 20-25% of the matrix mined was found to not be worth mining.

Table 4. Evaluation of the Pit Samples.

		P_2O_5	Fe_2O_3	Al_2O_3	MgO	CaO	% F	A.I.	Mine?
1	Lower	6.20	1.20	2.20	0.80	9.04	0.65	65.75	
4	Bottom	5.70	0.90	1.70	4.00	24.00	0.60	62.56	No
5	Upper Zone	7.90	1.10	3.80	0.90	11.53	0.83	62.71	
6	Upper	8.20	1.30	4.20	0.20	11.97	0.86	62.73	
7	Upper	10.80	0.60	3.40	0.20	15.76	1.13	67.06	
8	Upper	13.90	0.10	3.80	0.80	20.29	1.45	62.97	
9	Lower	8.42	1.30	2.20	0.65	12.29	0.88	63.81	
11	Upper	6.20	0.50	2.90	2.10	9.04	0.65	64.84	No
12	Upper	7.40	2.30	3.20	1.70	10.80	0.77	61.93	No
13	Upper	7.00	0.40	4.10	0.90	10.21	0.73	63.38	
14	Upper	8.90	0.60	2.90	0.70	12.99	0.93	62.13	
16	Upper	6.80	0.90	2.80	0.50	9.92	0.71	62.17	
17	Upper	8.10	1.00	3.30	0.70	11.82	0.85	75.89	
19	Lower	5.37	0.82	2.40	0.69	7.83	0.56	63.24	
20	Lower	5.52	0.97	2.30	0.72	8.05	0.58	64.20	
21	Lower	6.35	3.20	2.60	0.60	9.26	0.66	61.95	No
23	Upper	11.20	0.60	4.20	1.10	16.35	1.17	63.16	
24	Upper	6.10	0.50	4.40	0.90	8.90	0.64	64.79	
25	Lower	6.70	1.02	2.10	0.70	9.77	0.70	65.32	
26	Bottom	5.20	2.30	1.50	9.32	20.13	0.55	62.86	No
27	Upper	8.10	0.50	4.10	0.80	11.82	0.85	62.86	
28	Upper	9.70	0.70	5.20	0.60	14.16	1.01	63.14	
29	Upper	9.70	0.90	3.90	1.10	14.16	1.01	62.14	
30	Upper	10.30	0.70	4.20	0.69	15.03	1.07	64.20	

While it is highly probable that some of the materials that were not sent to the slurry pit (either cast aside as overburden or left in the mine cut) were good matrix, no samples were obtained of this material to confirm it. With just the improvement from not mining the matrix that should not have been mined, there is significant value. At an annual rock production rate of 4 million tons, and 5/24 of the matrix being mined and subsequently thrown away when it is caught by the MAYA on the pebble belt, the "wasted" cost can be significant. At a probable cost of $5/ton for mining, transporting, washing and screening the rock, the annual cost could be over $4,000,000. The rock that is not mined, but should have been (though not verified in this study) would add significantly more value.

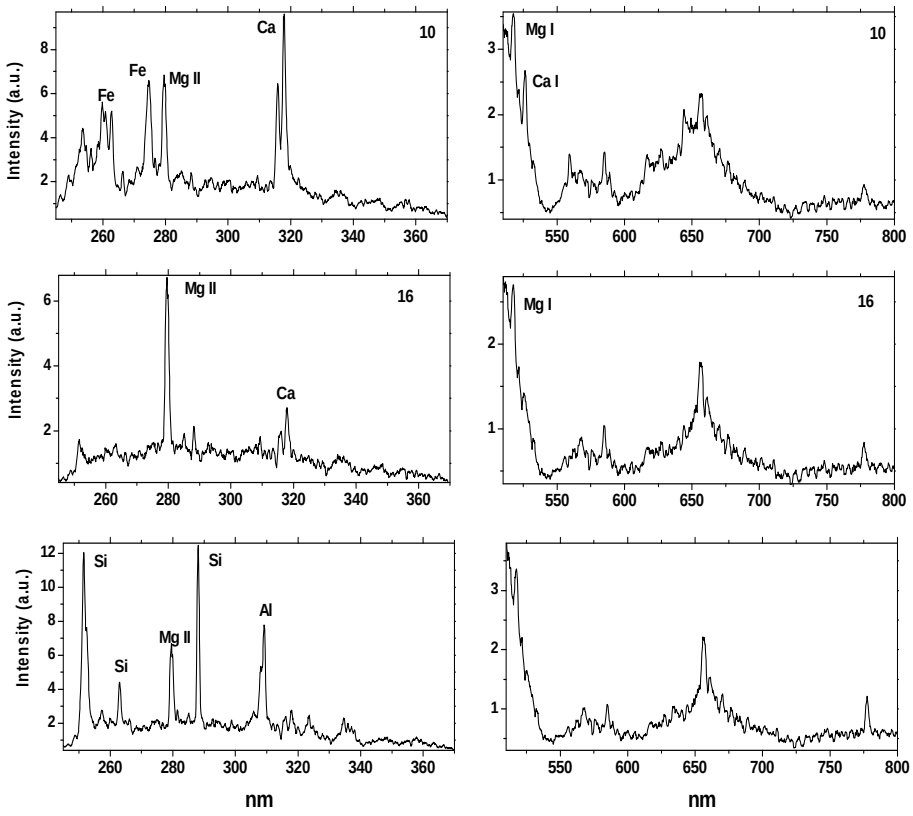

Figure 51. Breakdown Spectra with Very Low Ca Lines and Strong Emissions from Fe, Si, Mg and Al (Evidently Host Rocks).

FURTHER DISCUSSION

After the completion of the project, a meeting was held with the interested Mosaic personnel. While they accepted the value and reliability of the results, they re-questioned the optimum placement of the unit in the field. The location of the unit at the pumping pit was chosen mostly for safety reasons, but does require frequent moving of the unit and may be subject to significant splashing with mud from the pit guns. It was suggested that a better location and perhaps safer location is to mount the unit on the dragline boom so that it looks down at the area to be mined or on top of the dragline bucket as it is being

moved to the washing pit or spoil pile. While this will present technical challenges to compensate for vibration and movement of the boom, it would be of greater value to the mining operation as every bucket of material could be analyzed and immediately be available to the dragline operator.

CONCLUSIONS

An industrialized ReLIBS unit was developed and tested under field conditions. Compared to the previous efforts (FIPR 07-04-075) to develop a remote LIBS unit for the phosphate industry, the following changes were made:

1. The ReLIBS unit was made more rugged to make it capable of constantly working in the real-life conditions of an open phosphate mine with strong dust, wind and varying temperatures.
2. Scanning and auto-focusing abilities were added.
3. A double pulsed LIBS mode was used to substantially improve the signal/noise ratio.
4. Emission gating was reduced to 10 μs to minimize the strong sunlight interference.
5. Analytical performance was improved by including direct detection of P and the mineral apatite using the plasma emission of CaF molecules.
6. Field tests confirmed that ReLIBS enabled the realization of remote real time chemical analysis of phosphate ore as it was excavated by the dragline machine. It gives the following:

    a. Differentiation between overburden, matrix and bottom materials.
    b. Determination of the P_2O_5content.
    c. Determination of the MgO and iron content in matrix samples.

The following further technical improvements are suggested:

1. Improve the sensitivity in the visible range. The easiest way to do this is to use the wider spectral slit; for example, 200 μm instead the present 50 μm. The signal will be four times stronger. The resulting weaker spectral resolution may be compensated for by selection of the spectral grating with a higher number of lines/mm. It leads to a narrower spectral range, but is possible because the actual spectral range needed in this case is approximately 200 nm, or from 500 to 700 nm.
2. The green laser used to measure the distance and aiming the unit was not visible on the rocks at the 15-25 m distances in the bright Florida sun. Thus in many cases it was not possible to know the exact spot where the ReLIBS was shooting. LDS is planning to install four small but powerful green diode lasers on the laser shutter that will exactly define the small area where the laser beam will be focused.

REFERENCES

American National Standards Institute (ANSI). 2000. American national standard for the safe use of lasers: ANSI Z136.1. Orlando (FL): Laser Institute of America.

Cremers DL, Radziemski LJ. 2006. Handbook of laser-induced breakdown spectroscopy. Chichester (England): John Wiley & Sons.

Gaft M, Nagli L, Panczer G, Reisfeld R. 2002. Laser-induced luminescence and breakdown spectroscopy evaluation of phosphates with high dolomite content. In: Zhang P, El-Shall H, Somasundaran P, Stana R, eds. Beneficiation of phosphates: fundamentals and technology. Littleton (CO): SME. p 145-52.

Gaft M, Nagli L, inventors; Florida Institute of Phosphate Research, assignee. 2004 Jun 22. Mineral detection and content evaluation method. US Patent 6,753,957 B1.

Gaft M, Reisfeld R, Panczer G. 2005. Modern luminescence spectroscopy of minerals and materials. Berlin: Springer-Verlag.

Gaft M, Sapir-Sofer I, Stana R. 2007. Laser induced breakdown spectroscopy for bulk minerals online analyses. Spectrochimica Acta, Part B: Atomic Spectroscopy 62(12): 1496-1503.

Gaft M, Dvir E, Modiano H, Schone U. 2008. Laser induced breakdown spectroscopy machine for online ash analyses in coal. Spectrochimica Acta, Part B: Atomic Spectroscopy 63(10): 1177-82.

Gaft M, Nagli L. 2008. Laser-based spectroscopy for standoff detection of explosives. Optical Materials 30: 1739-46.

Gaft M, Nagli L, Fasaki I, Kompitsas M, Wilsch G. 2009. Laser-induced breakdown spectroscopy for on-line sulfur analyses of minerals in ambient conditions. Spectrochimica Acta, Part B: Atomic Spectroscopy 64(10): 1098-1104.

Gaft M, Nagli L, Groisman Y, Barishnikov A. 2014a. Industrial online raw materials analyzer based on laser-induced breakdown spectroscopy. Applied Spectroscopy 68(9): 1004-15.

Gaft M, Nagli L, Eliezer N, Groisman Y, Forni O. 2014b. Elemental analysis of halogens using molecular emission by laser-induced breakdown spectroscopy in air. Spectrochimica Acta Part B, Atomic Spectroscopy 98: 39-47.

Groisman Y, Gaft M. 2010. Online analysis of potassium fertilizers by laser-induced breakdown spectroscopy. Spectrochimica Acta, Part B: Atomic Spectroscopy 65(8): 744-9.

Miziolek A, Palleschi V, Schechter I. 2006. Laser-induced breakdown spectroscopy (LIBS): fundamentals and applications. Cambridge (UK): Cambridge University Press.

Noll R. 2012. Laser induced breakdown spectroscopy: fundamentals and applications. Berlin: Springer. 543 p.

Palanco S, Laserna J. 2004. Remote sensing instrument for solid samples based on open-path atomic emission spectrometry. Review of Scientific Instruments 75(6): 2068-74.

Sallé B, Mauchien P, Maurice S. 2007. Laser-induced breakdown spectroscopy in open-path configuration for the analysis of distant objects. Spectrochimica Acta, Part B: Atomic Spectroscopy 62(8): 739-68.